Electronic Supplementary Material (ESI) for Soft Matter.

Enhancement of the mechanical properties of lysine-containing peptide-based supramolecular hydrogels by chemical cross-linking

Libby J. Marshall,[a] Olga Matsarskaia,[b] Ralf Schweins[b] and Dave J. Adams[a]

[a]*School of Chemistry, University of Glasgow, Glasgow, G12 8QQ*

[b]*Institut Laue-Langevin, 71 Avenue des Martyrs, CS 20156,38042 Grenoble Cedex 9, France*

Supporting Information

Contents

1. Materials and Synthesis

All chemicals were purchased from Sigma Aldrich, Alfa, TCI and Fluorochem and used as received. The synthesis of the gelators studied here follow the same general methodology as previously described for similar compounds with slight differences to account for the solubility and reactivity of the starting materials.[1]

Peptide Coupling.

The compound with a free carboxylic acid group (the acid, 1 molar equivalent) was dissolved in $CHCl_3$ (20 mL/1 g of solid) with the addition of *N*-methyl morpholine (NMM, aliquots of 5 equivalents until a transparent solution was obtained). Isobutyl chloroformate (IBCF, 1.1 equivalents) was added and the solution stirred on ice for 10 minutes. The compound with a free amine group (the amine, 1 molar equivalent) was dissolved separately in $CHCl_3$ (20 mL/1 g of solid) with the addition of NMM (aliquots of 5 equivalents until a transparent solution was obtained). Following activation of the acid, the amine solution was added, and the reaction mixture stirred on ice overnight. The following day, the reaction mixture was washed sequentially with HCl (1 M, 1.25 x the volume of the reaction mixture), water (1.25 x the volume of the reaction mixture) and brine (1.25 x the volume of the reaction mixture). The organic phase was dried with $MgSO_4$, filtered and the solvent removed *in vacuo* to give the product. Where required, the product was purified by column chromatography in a 1:9 or 1:99 EtOAc :DCM solvent system, depending on separation from impurities on a TLC plate.

Boc Deprotection.

The Boc-protected peptide was dissolved in $CHCl_3$ (10 mL/1 g of solid) and trifluoroacetic acid (TFA) added such that the ratio of TFA:$CHCl_3$ was 1:2. The reaction was stirred overnight at room temperature before being poured into a large excess of Et_2O and stirred vigorously overnight. The resulting precipitate was filtered under vacuum to give the product as a solid. The product was dried further by azeotropic distillation with CH_3CN. Where required, the product was washed by trituration in Et_2O.

Methyl Ester Deprotection.

The methyl ester-protected peptide was dissolved in tetrahydrofuran (THF, 10 mL/1 g of solid). LiOH (5 molar equivalents) was dissolved separately in water so that the ratio of THF:water was 1:1. The LiOH solution was added to the peptide solution and the reaction stirred at room temperature. The reaction was monitored by TLC using a suitable solvent system (generally 1:9 EtOAc:DCM). After the reaction had gone to completion, the reaction mixture was poured into a large excess of 1 M HCl and stirred vigorously overnight. The resulting precipitate was filtered under vacuum, washed with plentiful deionised water and dried by azeotropic distillation with CH_3CN to give the product as a solid. Where required, the product was washed by trituration in Et_2O.

2. Experimental Details

Preparation of Stock Solutions.

Gelator solutions (10 mg/mL and 5 mg/mL) were prepared in Falcon Tubes by suspending the gelator in deionised water and adding two molar equivalents of sodium hydroxide solution (0.1 M, NaOH). The solutions were stirred for a minimum of 6 hours to ensure complete dissolution of the gelator. The pH of each solution was adjusted, if needed, to pH 11.6 ± 0.1 with either NaOH (1 M) or HCl (1M).

pH Measurements.

The pH of samples was measured using a FC200 pH probe from Hanna instruments. The probe was calibrated using pH 4, pH 7 and pH 10 buffers. The stated accuracy of the pH measurements is ± 0.1.

Preparation of gels.
Gel samples were prepared in Sterilin vials by addition of 2 mL of stock solution to 2.8 molar equivalents of glucono-δ-lactone (GdL). The vials were swirled briefly by hand to ensure complete dissolution of GdL then left to stand overnight undisturbed.

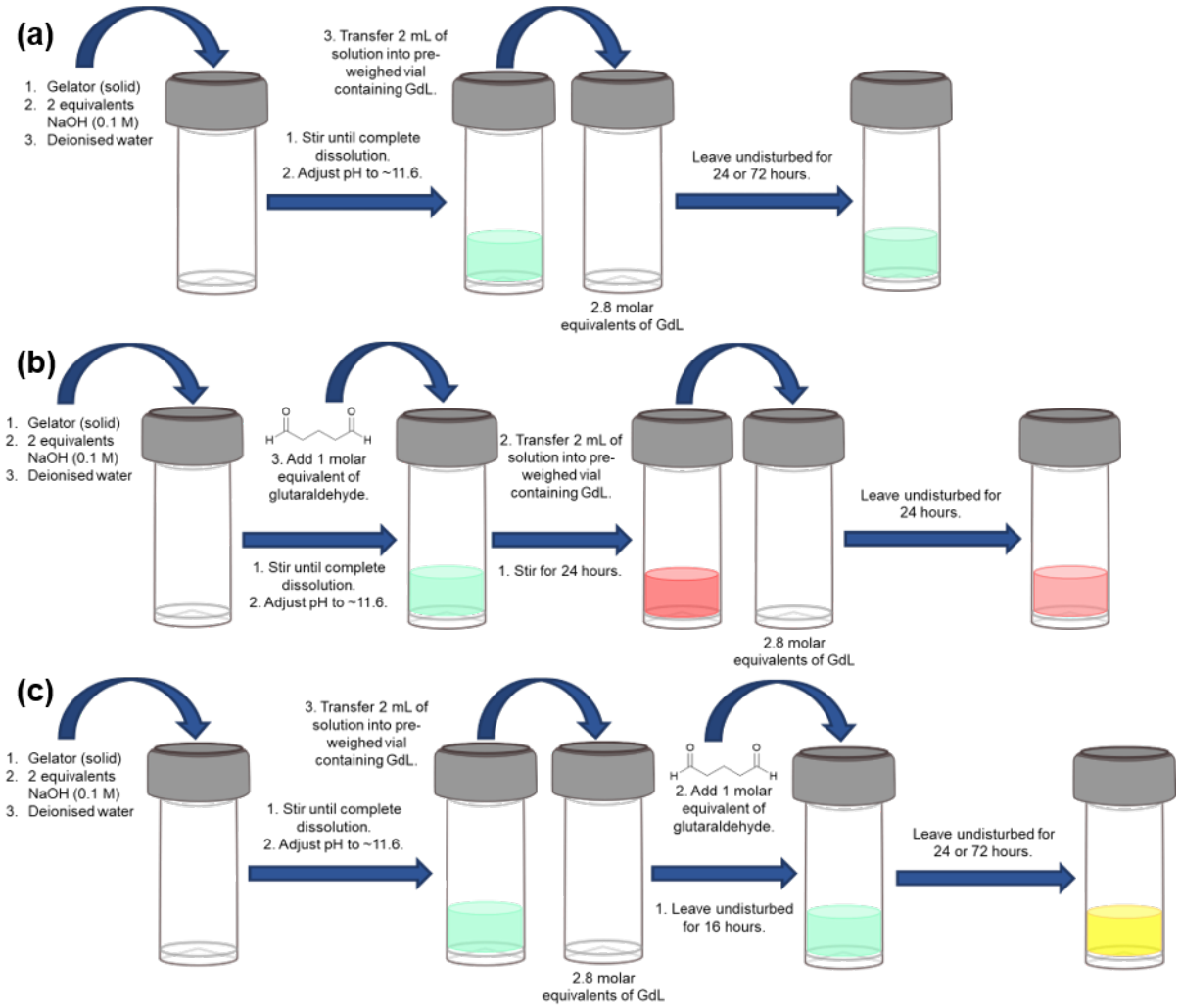

Figure S1. Schematic representations showing preparation of (a) control, (b) pre-gelation and (c) post-gelation samples.

Cross-linking with Glutaraldehyde.
For the post-gelation samples, the gels were prepared as previously described. After allowing gel formation overnight (~ 16 hours) glutaraldehyde (1 molar equivalent, in the form of 50 % aqueous solution) was pipetted on top of the pre-formed gels. The 24-hour and 72-hours samples were left to sit undisturbed for 24 hours and 72 hours respectively before rheology measurements were performed. For the pre-gelation samples, the gelators were stirred in solution with glutaraldehyde (1 molar equivalent) at pH 11.6 for 24 hours before gelation was triggered. After sitting overnight (~16 hours), these sample were left to sit undisturbed for a further 24 hours to ensure the samples were the same age as the 24-hour post-gelation and 24-hour control samples.

Viscosity.
Viscosity measurements were performed using an Anton Paar Physica MCR 101 rheometer at 25°C. Viscosity measurements were carried out on 10 mg/mL solutions of each tripeptide without glutaraldehyde at a pH ~11.5 and with 1 molar equivalent of glutaraldehyde using a 50 mm diameter cone and a plate

system. ~1 mL of solution was poured onto the plate. The viscosity of the solution was recorded under rotation shear rate varying from 1 to 1000 /s.

Rheology.
All rheological measurements were carried out using an Anton Paar Physica MCR 301 rheometer at 25 °C. Strain, frequency and time sweeps were performed using cup and vane geometry (ST10-4V-8.8/97.5-SN18190) with a gap height of 0.8 mm. Strain sweeps were performed at a frequency of 10 rad/s from 0.01% to 1000% strain. Frequency sweeps were performed at 0.1% strain from 1 rad/s to 100 rad/s frequency. Time sweeps were performed at 0.5% strain and 10 rad/s frequency. All samples were prepared as previously described in a 2 mL volume in 7 mL Sterilin vials.[2]

Small Angle Neutron Scattering.
Solutions were prepared as described above in D_2O using NaOD to adjust the pH. SANS measurements were performed using the D11 instrument (Institut Laue Langevin, Grenoble, France). A neutron beam, with a fixed wavelength of 6 Å and divergence of $\Delta\lambda/\lambda$ = 9%, allowed measurements over a large range in Q [$Q = 4\pi\sin(\theta/2)/\lambda$] range of 0.002 to 0.3 $Å^{-1}$, by using three sample-detector distances of 1.5 m, 8m, and 28 m.

Solutions and gels were measured in 2 mm path length UV spectrophotometer grade, quartz cuvettes (Hellma). These were placed in a temperature-controlled sample rack during the measurements. Gels formed using GdL were prepared in the cuvettes and then transferred to the rack.

The data were then reduced to 1D scattering curves of intensity vs. Q using the facility provided software. The electronic background was subtracted, the full detector images for all data were normalized and scattering from the empty cell was subtracted. The scattering from D_2O was also measured and subtracted from the data using the Mantid software package.[3] The instrument-independent data were then fitted to the models discussed in the text using the SasView software package version 5.0.3.[4]

Reduction with $NaBH_4$.
$NaBH_4$ (2 molar equivalents with respect to glutaraldehyde) was added as a solid to the selected samples. The high pH sample was stirred for 16 hours while the gel samples were left to sit undisturbed while the reaction was monitored over 24 hours.

3. Viscosity data.

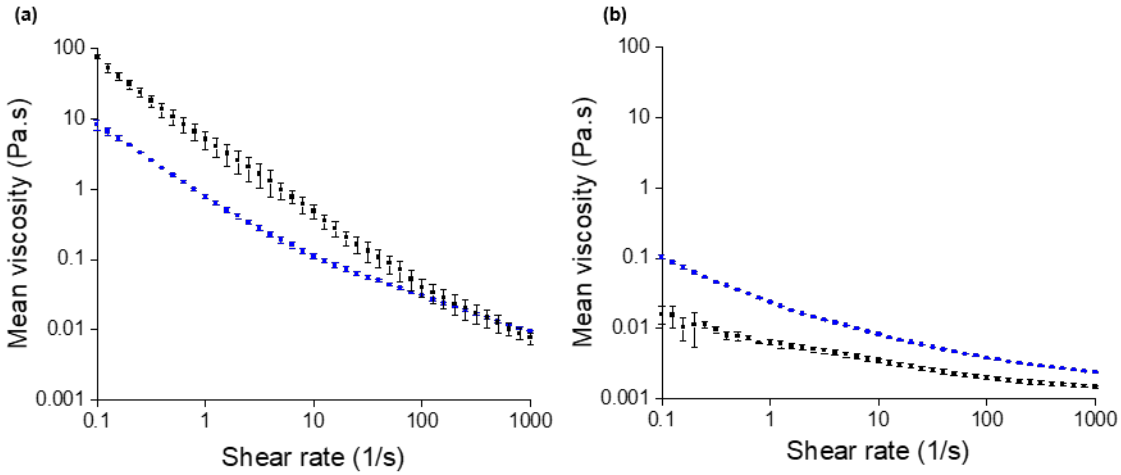

Figure S2. Average viscosity was calculated from three samples of solutions of 2NapFFK (blue), 2NapKFF (black) at concentrations of 10 mg/mL. Error bars were calculated from the standard deviation between the three samples **(a)** without glutaraldehyde at pH ~11.5 **(b)** stirred with 1 molar equivalent of glutaraldehyde for 24 hours without pH adjustment to replicate conditions in pre-gelation gels (pH >11.0).

Viscosity measurements show that both 2NapFFK (blue) and 2NapKFF (black) display shear thinning behaviour in aqueous solution at pH 11.6 (Figure S2a), indicative of the presence of worm-like micelles. Stirring with glutaraldehyde (Figure S2b) results in decreased viscosity, showing the presence of glutaraldehyde affects the structures formed by these gelators in solution at high pH. However, the shear-thinning behaviour persists, showing long one-dimensional structures are still present.

4. Rheology Data.

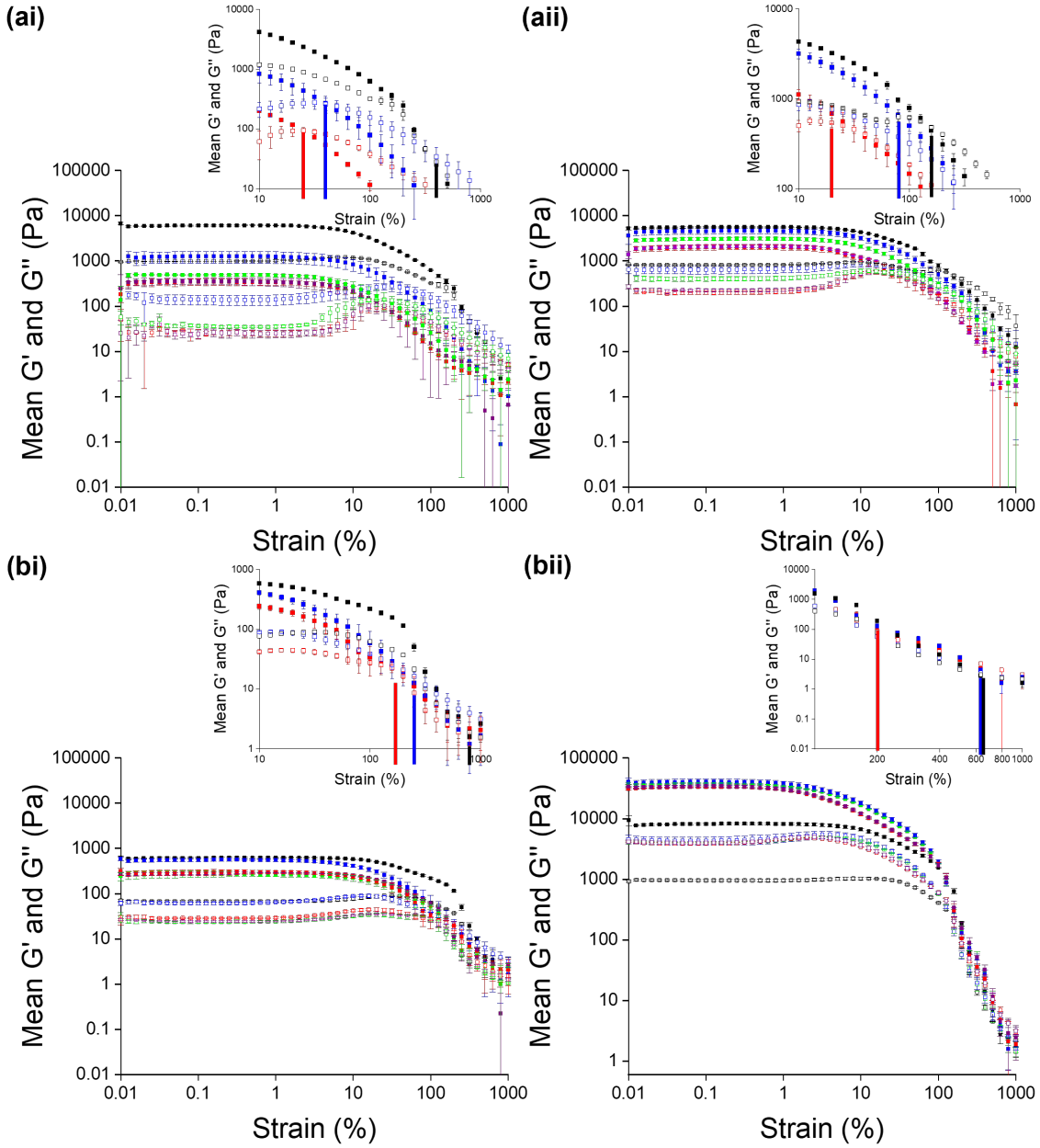

Figure S3. Strain sweeps collected from samples of (a) 2NapFFK and (b) 2NapKFF at concentrations of (i) 5 mg/mL and (ii) 10 mg/mL with glutaraldehyde added pre-gelation (black), glutaraldehyde added post-gelation and left to react for 24 hours (green), glutaraldehyde added post-gelation and left to react for 72 hours (blue), 24-hour controls without glutaraldehyde (red) and 72-hour controls without glutaraldehyde (purple). G' (filled squares) and G" (empty squares) were calculated from the average of three samples. Error bars show the standard deviation between the three samples. The inserts show an expanded view of the section of the strain sweep where G' and G" cross over one-another in the 24-hour controls, 72-hour post-gelation samples and the pre-gelation samples. These values were used to calculate the cross-over point of the gels.

2NapFFK shows similar changes in rheological properties at both concentrations. At 10 mg/mL, 2NapKFF (Figure S2b) showed very little difference between the 24-hour (green) and 72-hour (blue) post gelation samples. It could be that more time is needed at a higher concentration for this gelator to interact with glutaraldehyde, owing to a denser gel network, or that the maximum increase in gel properties had already been reached within 24-hours. Interestingly, the post-gelation samples showed higher G' values but same G" values as control samples, suggesting greater elasticity. Slight increases in the length of the linear viscoelastic region were also observed, showing increased gel strength. The pre-gelation samples (black) showed decreased G' and G" but a considerable increase in the linear viscoelastic region, suggesting that while exposure to glutaraldehyde pre-gelation reduced the stiffness of the gels, their resistance to strain was increased. This change of properties is in opposition to what is usually seen following chemical cross-linking.

We also investigated the effect of time allowed for the cross-linking reaction to take place on the post gelation samples (Figure S4). The post-gelation and control samples were prepared as described above and left for 3, 6 and 10 days. The control samples on each day were very similar. Hence, only one set of control samples is included for simplicity. The rheology of the 3-day and 6-day post-gelation samples are almost identical. There is a very slight increase in the stiffness (G') of the 10-day samples. However, leaving the samples for this long introduces more margins for change outside cross-linking, such as changes in temperature and degradation of the gel network with time, making leaving samples for this length of time unappealing. We therefore kept the maximum number of days for the post-gelation samples at 3 days.

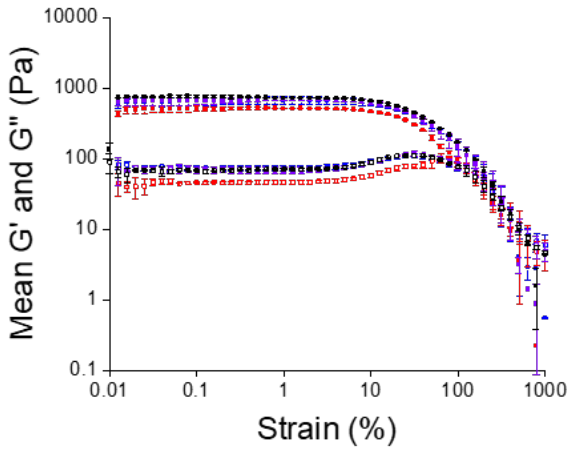

Figure S4. Samples prepared from 2NapFFK at a concentration of 5 mg/mL with no GTA (red), and GTA added post-gelation and left to react for 3 days (blue), 6 days (purple) and 10 days (black) before rheology measurements. Rheology was performed in triplicate in each condition. Error bars show the standard deviation between the three samples in each condition.

We also investigated the effect of GTA concentration on the outcome of cross-linking pre-gelation.

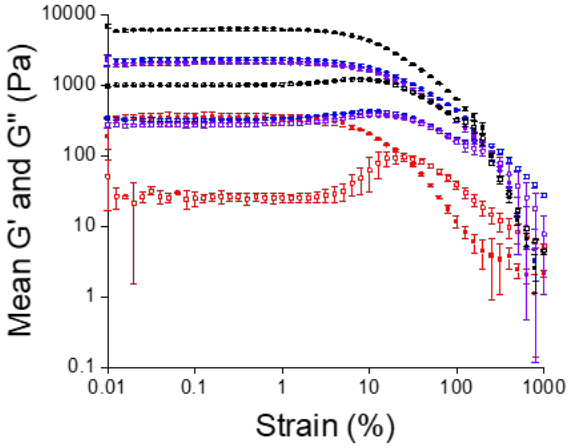

Figure S5. Samples prepared from 2NapFFK at a concentration of 5 mg/mL as described above. The control samples (no GTA) are shown in red. GTA was added pre-gelation to the remaining samples at molar ratios of glutaraldehyde:2NapFFK of, 1:1, (as in main text, black), 1:2 (blue), and 1:5 (purple). Rheology was performed in triplicate in each condition. Error bars show the standard deviation between the three samples in each condition. While lower molar ratios of glutaraldehyde to 2NapFFK gave the same increase in strength (where G' crosses over G", the increase in stiffness was not as great as at a molar ratio of 1:1. We hence used a molar ratio of 1:1 in all other conditions. It is likely that glutaraldehyde is reacting in polymeric form and hence several glutaraldehyde molecules will be required to form a single cross-link.

All frequency sweeps (shown on the following pages) are in good agreement with the G' and G" values recorded in the corresponding strain sweeps, showing good reproducibility between samples.

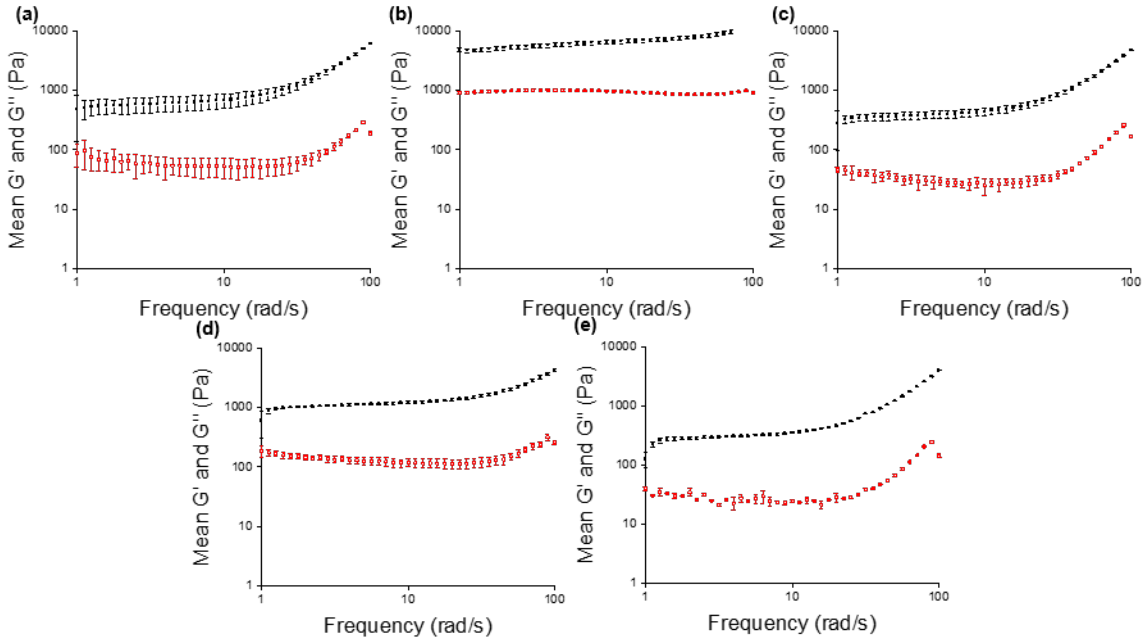

Figure S6. Frequency sweeps of 2NapFFK at 5 mg/mL with (a) glutaraldehyde added to gel post-gelation and left to react for 24 hours (b) glutaraldehyde stirred in solution with gelator at pH 11.6 for 24 hours pre-gelation, (c) no glutaraldehyde (control for 24-hour post-gelation and pre-gelation samples), (d) glutaraldehyde added to gel post-gelation and left to react for 72 hours, (e) no glutaraldehyde (control for 72-hour post-gelation samples). Mean G' (black) and G" (red) were calculated from three samples. The error bars show the standard deviation between samples.

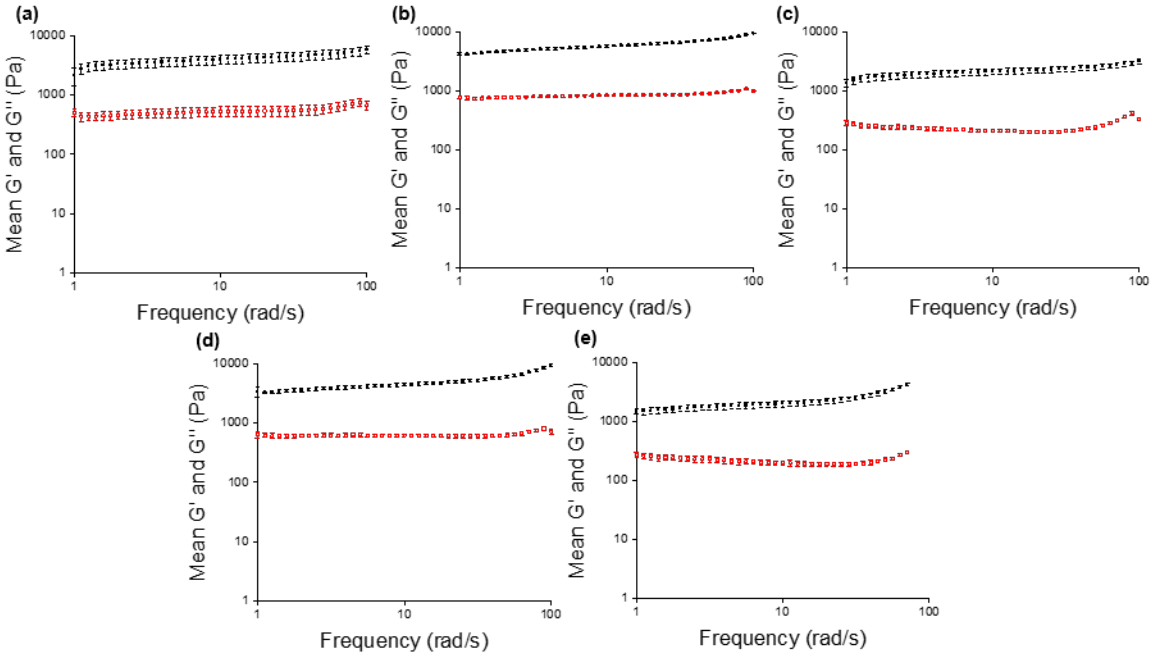

Figure S7. Frequency sweeps of 2NapFFK at 10 mg/mL with (a) glutaraldehyde added to gel post-gelation and left to react for 24 hours (b) glutaraldehyde stirred in solution with gelator at pH 11.6 for 24 hours pre-gelation, (c) no glutaraldehyde (control for 24-hour post-gelation and pre-gelation samples), (d) glutaraldehyde added to gel post-gelation and left to react for 72 hours, (e) no glutaraldehyde (control for 72-hour post-gelation samples). Mean G' (black) and G" (red) were calculated from three samples. The error bars show the standard deviation between samples.

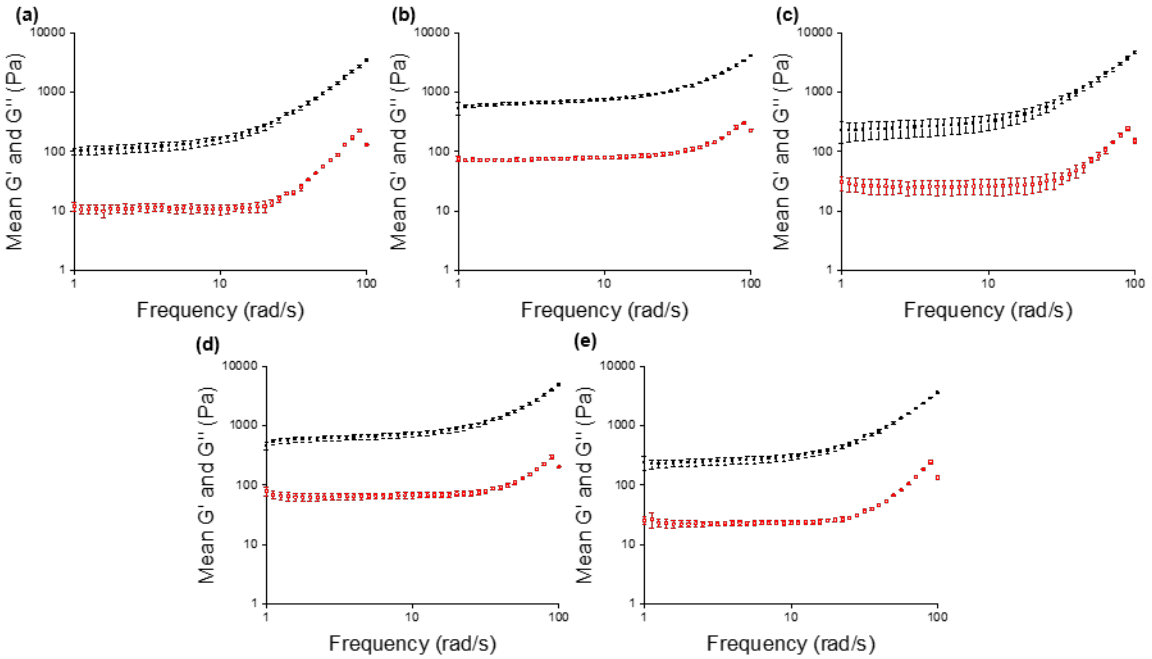

Figure S8. Frequency sweeps of 2NapKFF at 5 mg/mL with (a) glutaraldehyde added to gel post-gelation and left to react for 24 hours (b) glutaraldehyde stirred in solution with gelator at pH 11.6 for 24 hours pre-gelation, (c) no glutaraldehyde (control for 24-hour post-gelation and pre-gelation samples), (d) glutaraldehyde added to gel post-gelation and left to react for 72 hours, (e) no glutaraldehyde (control for 72-hour post-gelation samples). Mean G' (black) and G" (red) were calculated from three samples. The error bars show the standard deviation between samples.

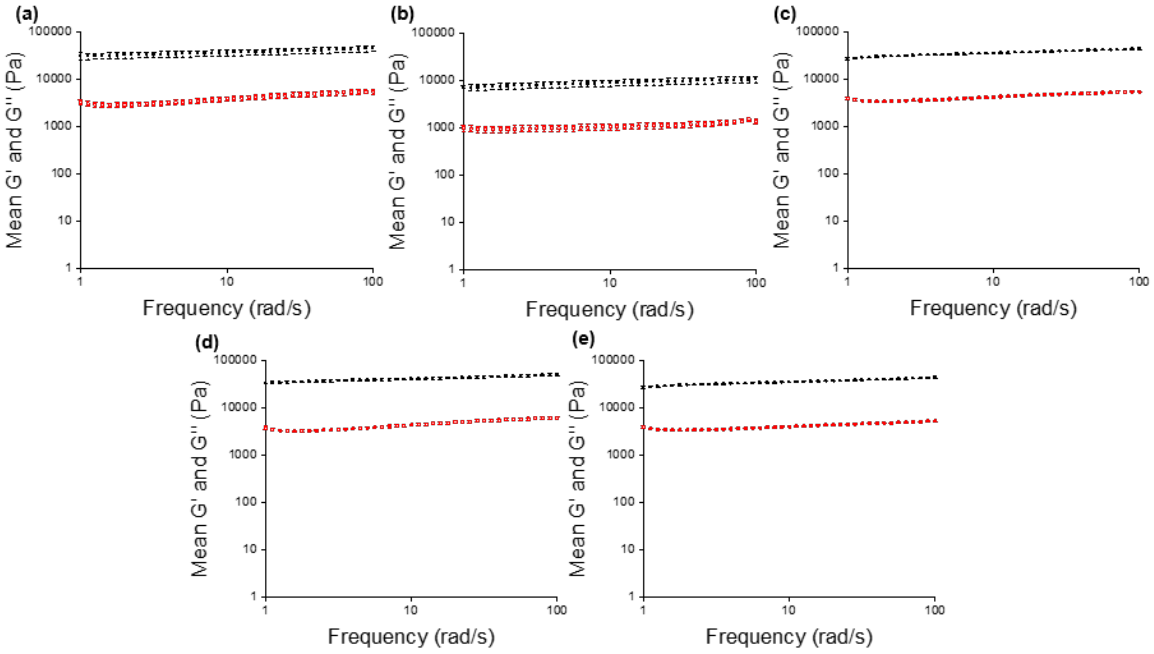

Figure S9. Frequency sweeps of 2NapKFF at 10 mg/mL with (a) glutaraldehyde added to gel post-gelation and left to react for 24 hours (b) glutaraldehyde stirred in solution with gelator at pH 11.6 for 24 hours pre-gelation, (c) no glutaraldehyde (control for 24-hour post-gelation and pre-gelation samples), (d) glutaraldehyde added to gel post-gelation and left to react for 72 hours, (e) no glutaraldehyde (control for 72-hour post-gelation samples). Mean G' (black) and G" (red) were calculated from three samples. The error bars show the standard deviation between samples.

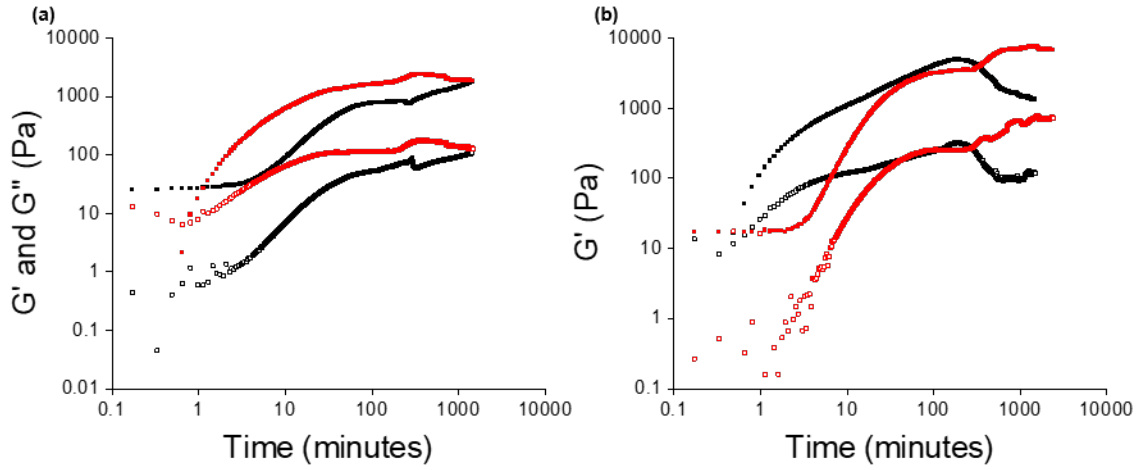

Figure S10. Time sweeps of 2NapFFK at (a) 5 mg/mL and (b) 10 mg/mL. The samples stirred with glutaraldehyde at pH 11.6 for 24 hours before triggering gelation and starting the time sweep are shown in black. The control samples without any glutaraldehyde are shown in red. Filled data points are G' and empty data points are G". G' and G" increase with time as the gelators self-assemble and the gel network forms. G' and G" reach a plateau once the gel network has fully formed and not further self-assembly is taking place. Interestingly, the samples with glutaraldehyde show a further increase in G' and G" after this plateau has been reached, suggesting cross-linking is still taking place and enhancing the stiffness of the gels.

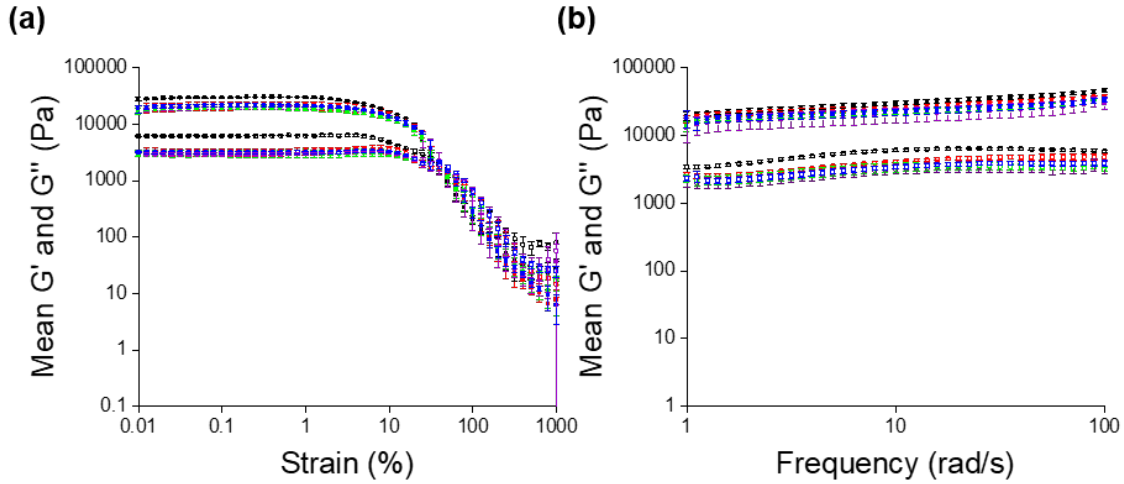

Figure S11. (a) Strain sweeps and (b) frequency sweeps collected from samples of 2NapFF at a concentration 5 mg/mL with glutaraldehyde added pre-gelation (black), glutaraldehyde added post-gelation and left to react for 24 hours (green), glutaraldehyde added post-gelation and left to react for 72 hours (blue), 24 hour controls without glutaraldehyde (red) and 72 hour controls without glutaraldehyde (purple). Mean G' (filled squares) and G" (empty squares) were calculated from the average of three samples. Error bars show the standard deviation between the three samples.

Figure S9 shows that addition of glutaraldehyde to gels formed from 2NapFF (a well-known, peptide-based supramolecular gelator without a lysine residue) does not change the rheological properties of the gels. This agrees with our hypothesis that the changes in mechanical properties observed in 2NapFFK and 2NapKFF is due to cross-linking between neighbouring lysine residues via glutaraldehyde molecules. Stirring 2NapFF with glutaraldehyde prior to gelation does result in slight changes in the rheological properties of the gels. It is postulated that the glutaraldehyde molecules are disturbing the self-assembly process as the gels formed had smaller tanδ values, showing reduced elasticity. Similar behaviour has been observed when exposing supramolecular hydrogelators to hydrophilic additives such as dextran.

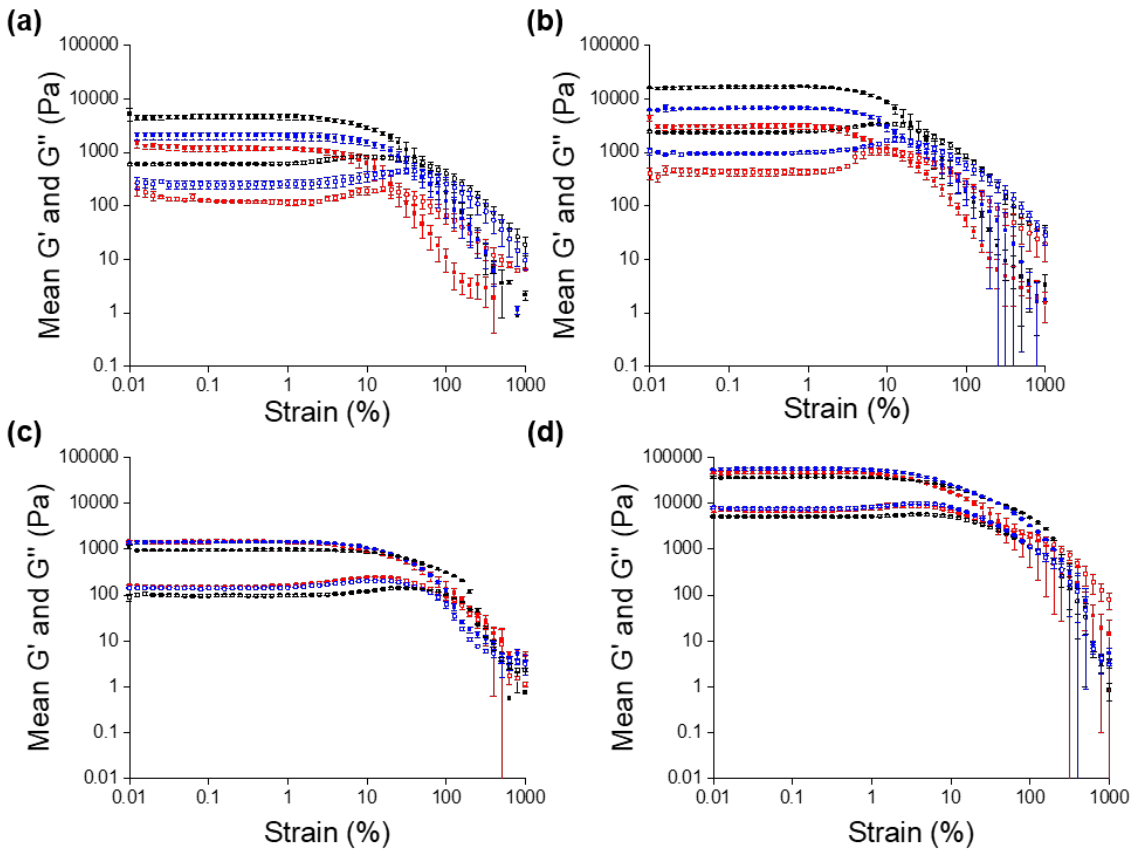

Figure S12. Strain sweeps of samples prepared in D_2O of (a) 2NapFFK (5 mg/mL), (b) 2NapFFK (10 mg/mL), (c) 2NapKFF (5 mg/mL) and (d) 2NapKFF (10 mg/mL) with glutaraldehyde added pre-gelation (black), glutaraldehyde added post-gelation and left to react for 72 hours (blue) and control gels with no glutaraldehyde (red). G' (filled squares) and G" (hollow squares) were calculated from the average of three samples. Error bars show the standard deviation between samples.

2NapFFK showed the same changes in behaviour with cross-linking pre- and post-gelation in D_2O as in H_2O at both concentrations examined here, showing that data collected from small-angle neutron scattering (SANS) of gels prepared in D_2O can be extrapolated to the behaviour in H_2O. SANS is performed in deuterated solvents to allow sufficient contrast for meaningful data to be collected. 2NapKFF shows similar behaviour in D_2O as in H_2O. G' and G" decrease slightly at both 5 mg/mL and 10 mg/mL, but to a much lesser extent than at 10 mg/mL in H_2O. Cross-linking post-gelation still results in an increase in both G' and G" at both concentrations of 2NapKFF. Importantly, the linear viscoelastic regions of the cross-linked gels still notably increase for both gelators at both concentrations, showing cross-linking still imparts increased gel strength in D_2O. Again, the frequency sweeps (shown on the following pages are in excellent agreement with the strain sweeps).

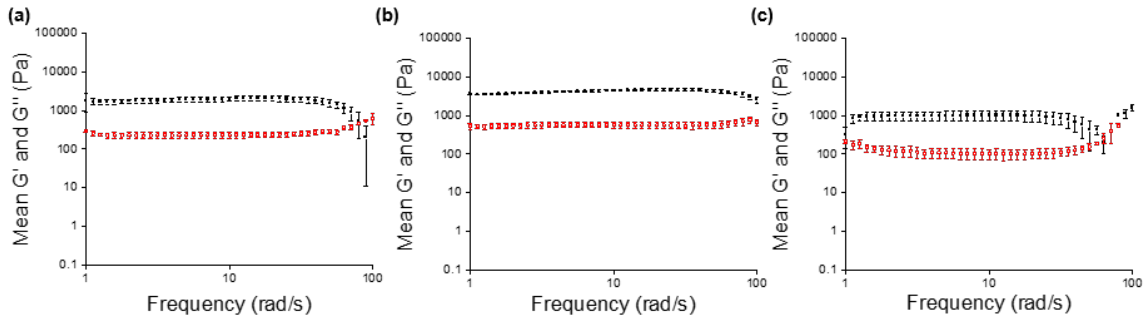

Figure S13. Frequency sweeps from samples of 2NapFFK (5 mg/mL) prepared in D_2O (a) with glutaraldehyde added post-gelation, (b) with glutaraldehyde added pre-gelation and (c) with no glutaraldehyde. Mean G' (black) and G'' (red) were calculated from three samples. The error bars show the standard deviation between the three samples.

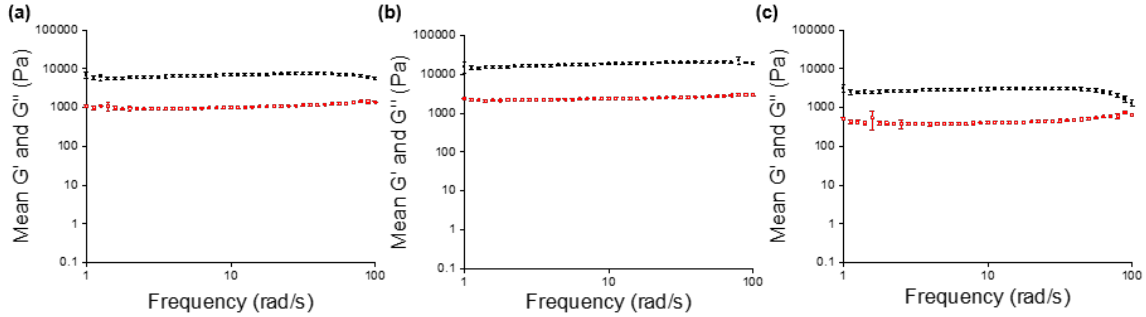

Figure S14. Frequency sweeps from samples of 2NapFFK (10 mg/mL) prepared in D_2O (a) with glutaraldehyde added post-gelation, (b) with glutaraldehyde added pre-gelation and (c) with no glutaraldehyde. Mean G' (black) and G'' (red) were calculated from three samples. The error bars show the standard deviation between the three samples.

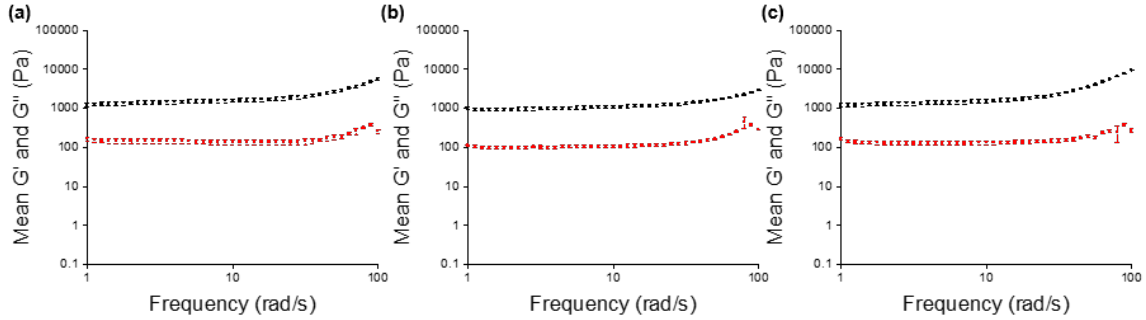

Figure S15. Frequency sweeps from samples of 2NapKFF (5 mg/mL) prepared in D_2O (a) with glutaraldehyde added post-gelation, (b) with glutaraldehyde added pre-gelation and (c) with no glutaraldehyde. Mean G' (black) and G'' (red) were calculated from three samples. The error bars show the standard deviation between the three samples.

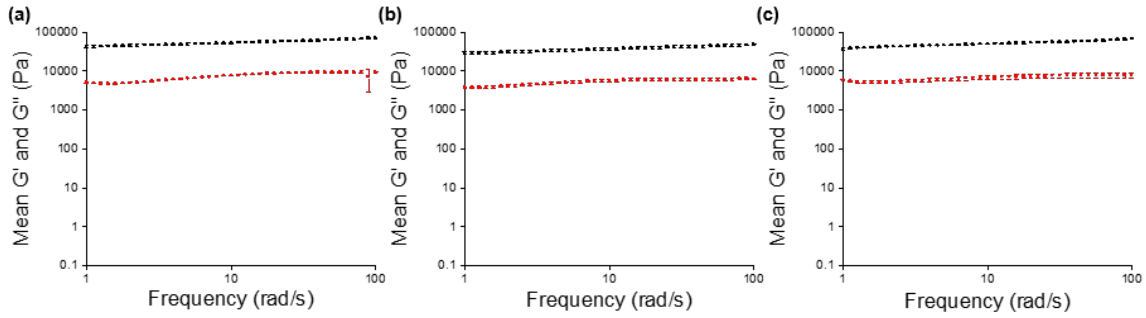

Figure S16. Frequency sweeps from samples of 2NapKFF (10 mg/mL) prepared in D_2O (a) with glutaraldehyde added post-gelation, (b) with glutaraldehyde added pre-gelation and (c) with no glutaraldehyde. Mean G' (black) and G'' (red) were calculated from three samples. The error bars show the standard deviation between the three samples.

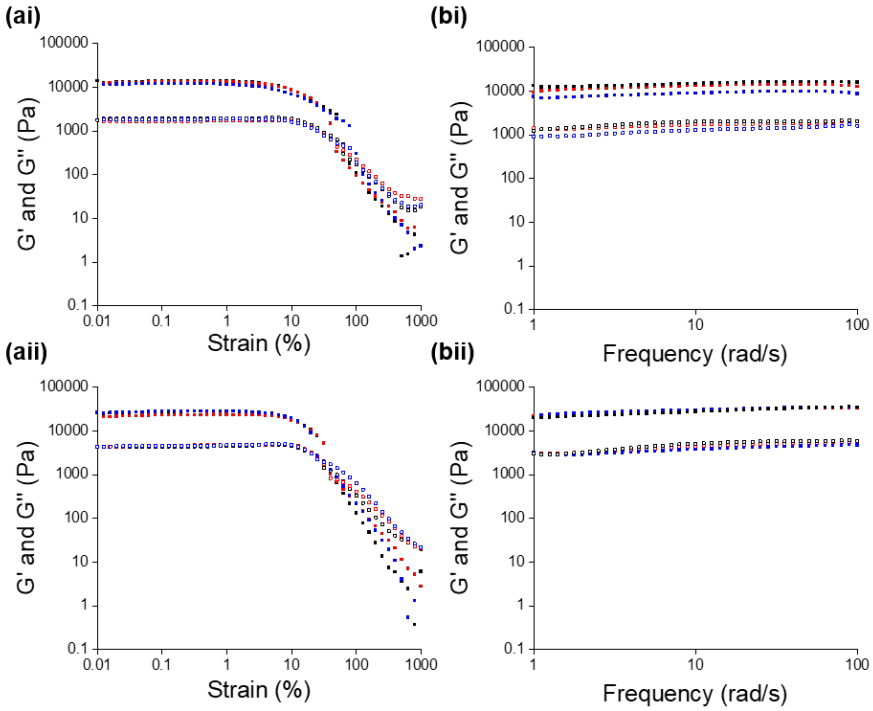

Figure S17. (a) Strain sweeps and (b) frequency sweeps of samples prepared in D_2O of 2NapFF at concentrations of (i) 5 mg/mL) and (ii) 10 mg/mL with glutaraldehyde added pre-gelation (black), glutaraldehyde added post-gelation and left to react for 72 hours (blue) and control gels with no glutaraldehyde (red). G' (filled squares) and G'' (hollow squares).

As in H_2O, 2NapFF shows no considerable changes in rheological behaviour on exposure to glutaraldehyde in D_2O, illustrating that cross-linking is taking place via the amine groups on the lysine residues of 2NapFFK and 2NapKFF. We therefore expected that the data collected from SANS of samples of 2NapFF exposed to glutaraldehyde would be very similar to the control samples without any glutaraldehyde.

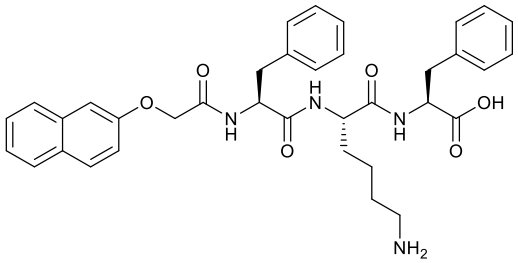

Figure S18. Chemical structure of the gelator 2NapFKF.

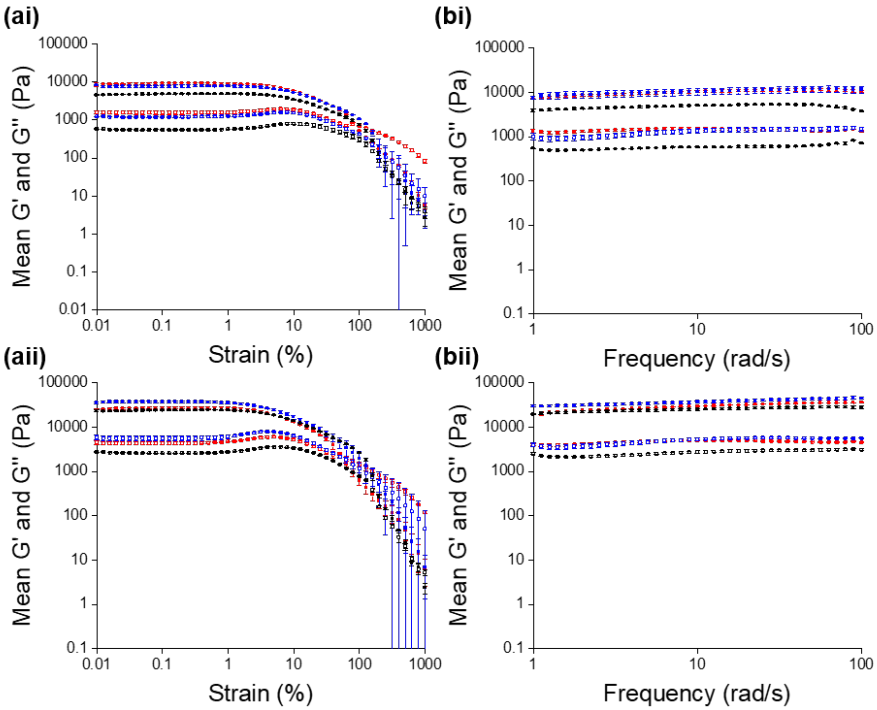

Figure S19. (a) Strain sweeps and (b) frequency sweeps of samples prepared in H_2O of 2NapFKF at concentrations of (i) 5 mg/mL) and (ii) 10 mg/mL with glutaraldehyde added pre-gelation (black), glutaraldehyde added post-gelation and left to react for 72 hours (blue) and control gels with no glutaraldehyde (red). Mean G' (filled squares) and G" (hollow squares) were calculated from the average values obtained from three samples in each condition. The error bars show the standard deviation between the three samples in each condition. Note that all strain and frequency sweeps were recorded from fresh samples.

Figure S19 shows that cross-linking post-gelation does not greatly affect the rheological properties of 2NapFKF at a concentration of 5 mg/mL. At a concentration of 10 mg/mL, cross-linking post-gelation resulted in inceased G' and G" as well as a slightly increased gel strength, similar to the behaviour seen with both 2NapKFF and 2NapFFK. Cross-linking 2NapFKF pre-gelation resulted in decreased G' and G" as well as increased gel strength, similar to the behaviour observed with 2NapKFF.

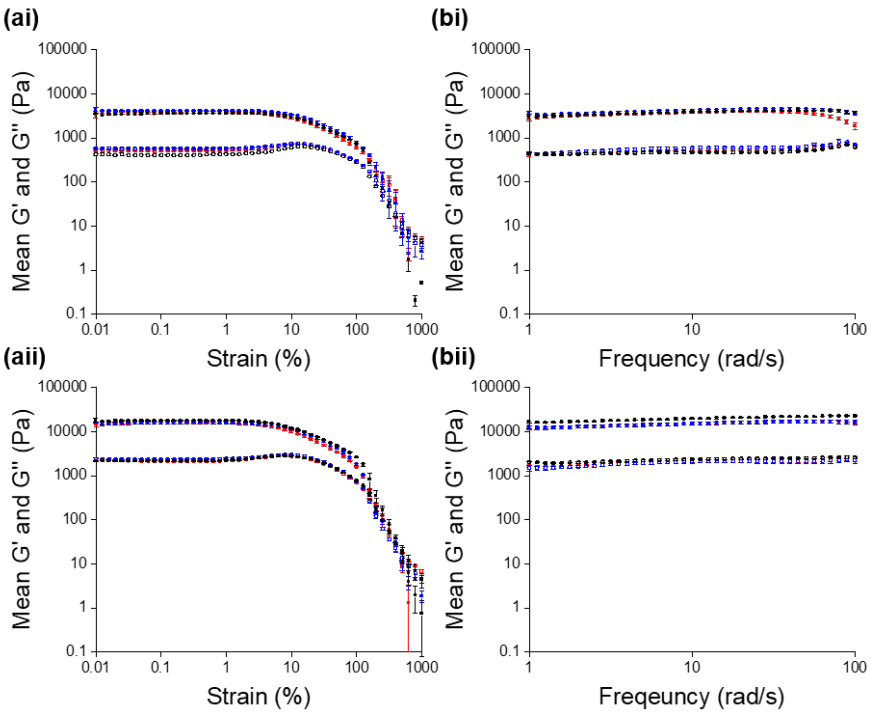

Figure S20. (a) Strain sweeps and (b) frequency sweeps of samples prepared in D_2O of 2NapFKF at concentrations of (i) 5 mg/mL) and (ii) 10 mg/mL with glutaraldehyde added pre-gelation (black), glutaraldehyde added post-gelation and left to react for 72 hours (blue) and control gels with no glutaraldehyde (red). G' (filled squares) and G'' (hollow squares).

Cross-linking in D_2O had limited effects on the properties of 2NapFKF, other than increasing tanδ (G''/G') and frequency independence. It is postulated that the K residues are harder to access in the structures formed by 2NapFKF compared to 2NapFFK and 2NapKF, resulting in only slight reinforcement of the gel network.

5. Small angle neutron scattering

The fits shown were selected on the basis of lowest chi2, as well as reasonable values for each parameter. It is noted that this model does not capture the data perfectly at 0.02 Q.

Condition	No GTA	GTA pre-gelation	GTA post-gelation
Cylinder scale	0.0015	0.0017	0.0013
Cylinder scale error	4.48 e^{-06}	1.22 e^{-05}	1.14 e^{-05}
Background (cm^{-1})	0.011	0.012	0.027
Background error (cm^{-1})	3.47e^{-05}	3.66 e^{-05}	4.07 e^{-05}
Radius (A°)	14.8	18.0	32.0
Radius error (A°)	0.02	0.69	0.37
Radius polydispersity	0.10	0.81	0.26
Radius polydispersity error	1.84 e^{-09}	0.05	0.01
Length (A°)	1119	401	1254
Length error (A°)	37.75	4.32	45.04
SLD (e^{-06} A°)	2.176	2.176	2.176
Solvent SLD (e^{-06} A°)	6.31	6.31	6.31
Power law scale	7.74 e^{-06}	1.47 e^{-05}	4.32 e^{-05}
Power law scale error	3.75 e^{-07}	7.98 e^{-07}	1.07 e^{-06}
Power law	2.67	2.61	2.39
Power law error	0.009	0.010	0.010
Reduced Chi^2	**8.71**	**8.01**	**10.88**

Table S1. Fitting parameters obtained from SasView model fitting of the SANS data. Parameter errors are fitting errors.

All three data sets were fit to a cylinder model combined with a power law model. Polydispersity was also included for the radius which improved the fit, suggesting more than one population of fibres was present in each samples. The pre-gelation sample was undoubtedly best fit to the chosen model. The control and post-gelation samples gave similar chi^2 values when fit to an elliptical cylinder model combined with a power law as when fit to the chosen model. However, in the case of the control sample, the elliptical cylinder model gave an axis ratio of ~1 when fit to the elliptical cylinder model, showing the fibres are not elliptical. For the post-gelation sample, the elliptical cylinder combined with a power law model did not fit the data as well at high Q as with the cylinder combined with a power law model. It could be that cross-linking of two adjacent fibres gave the impression of an elliptical cylinder with an axis ratio of 2.

6. Proof of Imine formation.

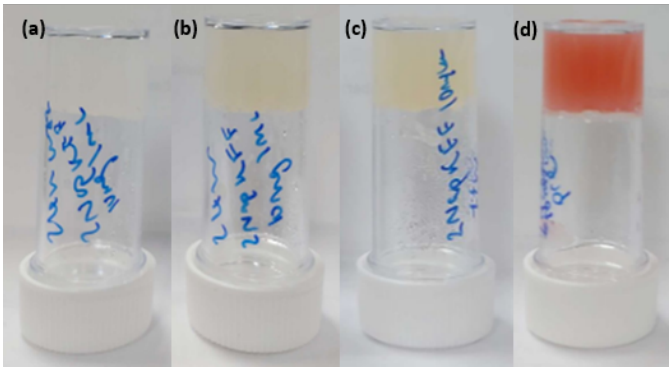

Figure S21. Photographs of gels formed from 2NapKFF at a concentration of 10 mg/mL (a) without glutaraldehyde, (b) after cross-linking with glutaraldehyde for 24 hours post-gelation, (c) after cross-linking with glutaraldehyde for 72 hours post-gelation, and (d) after stirring with glutaraldehyde for 24 hours pre-gelation. The same colour changes were observed in all other systems. All samples were prepared with a volume of 2 mL in 7 mL Sterilin vials.

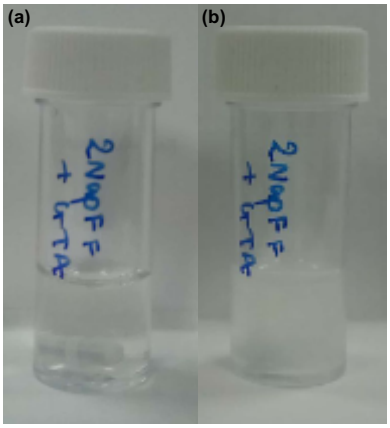

Figure S22. Photographs of a solution of 2NapFF (5 mg/mL) at pH 11.6 (a) before and (b) after stirring with glutaraldehyde for 24 hours. The solution was prepared with a volume of 2 mL in a 7 mL Sterilin vial. No colour change was observed on stirring with glutaraldehyde, confirming no imine formation without a lysine residue.

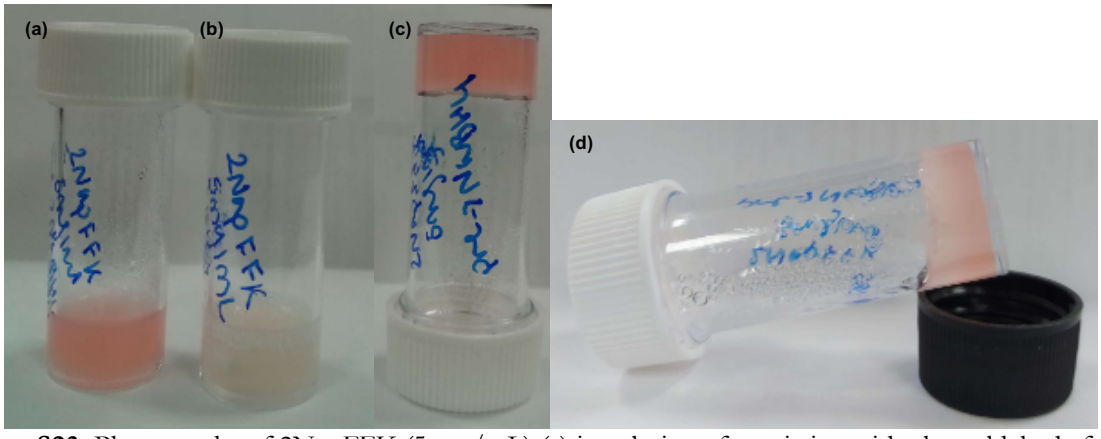

Figure S23. Photographs of 2NapFFK (5 mg/mL) (a) in solution after stirring with glutaraldehyde for 24 hours at pH 11.6, (b) in solution after stirring for 24 hours at pH 11.6 then stirring with $NaBH_4$ for 16 hours, showing loss of colour and therefore reversal of imine formation, (c) as a gel exposed to glutaraldehyde pre-gelation, (d) the same gel after exposure to $NaBH_4$, showing loss of colour change and disruption of the gel on reduction of the imine bonds. All samples had a volume of 2 mL and were prepared in 7 mL Sterilin vials.

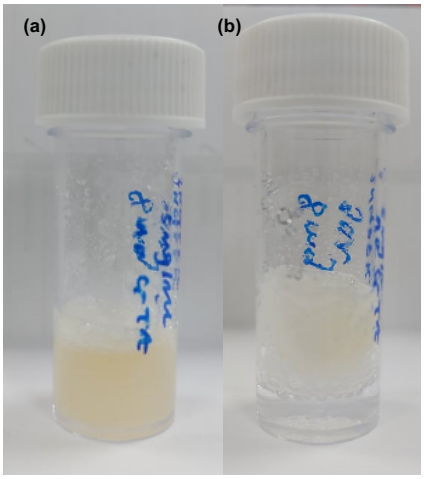

Figure S24. Photographs of a gel formed from 2NapFFK with a concentration of 5 mg/mL (a) exposed to glutaraldehyde post-gelation on addition of $NaBH_4$ and (b) the same gel after reacting $NaBH_4$ for 24 hours resulted in syneresis and loss of the yellow colour change. The sample was prepared with a volume of 2 mL in a 7 mL Sterilin vial.

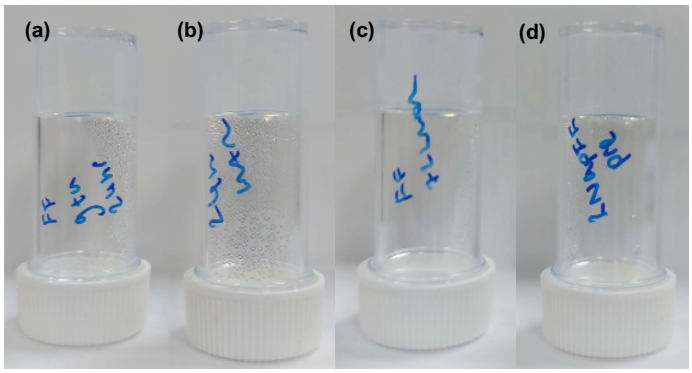

Figure S25. Photographs of gels formed from 2NapFF at a concentration of 5 mg/mL **(a)** without glutaraldehyde, **(b)** after cross-linking with glutaraldehyde for 24 hours post-gelation, **(c)** after cross-linking with glutaraldehyde for 72 hours post-gelation, **(d)** after stirring with glutaraldehyde for 24 hours pre-gelation. No colour change was observed, confirming no imine bond formation, as expected. All samples were prepared with a volume of 2 mL in 7 mL Sterilin vials.

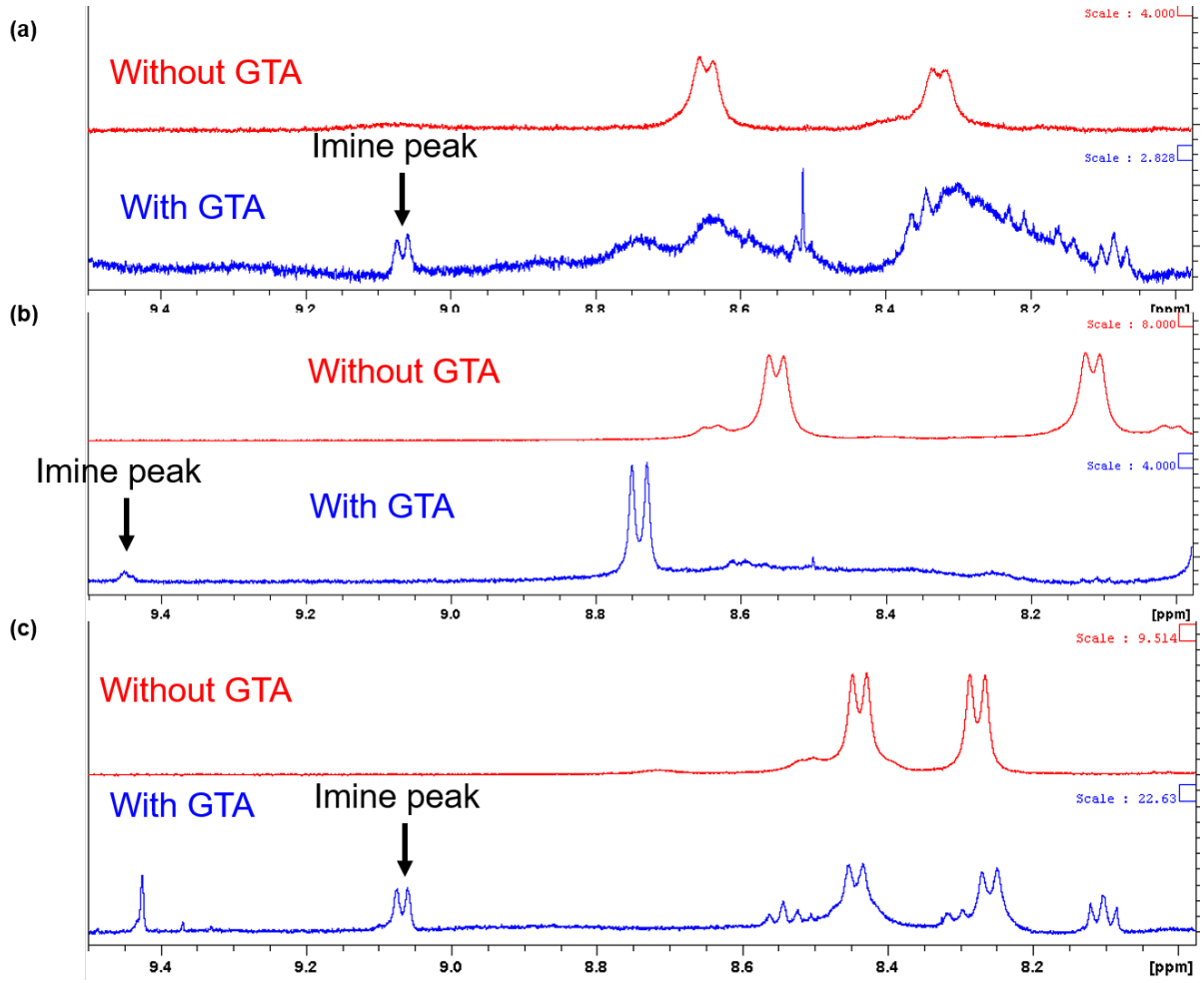

Figure S26. Expansion of ^{1}H NMR spectra of samples of **(a)** 2NapFFK, **(b)** 2NapKFF and **(c)** 2NapFKF without glutaraldehyde (red) and after stirring with glutaraldehyde at pH 11.6 for 24 hours (blue). The samples were prepared as aqueous solutions at pH 11.6 then freeze-dried. $DMSO_{d6}$ was used as the solvent for NMR spectroscopy.

The NMR spectra of the cross-linked samples clearly show the presence of an imine peak, confirming cross-linking is taking place via imine formation between lysine residues.

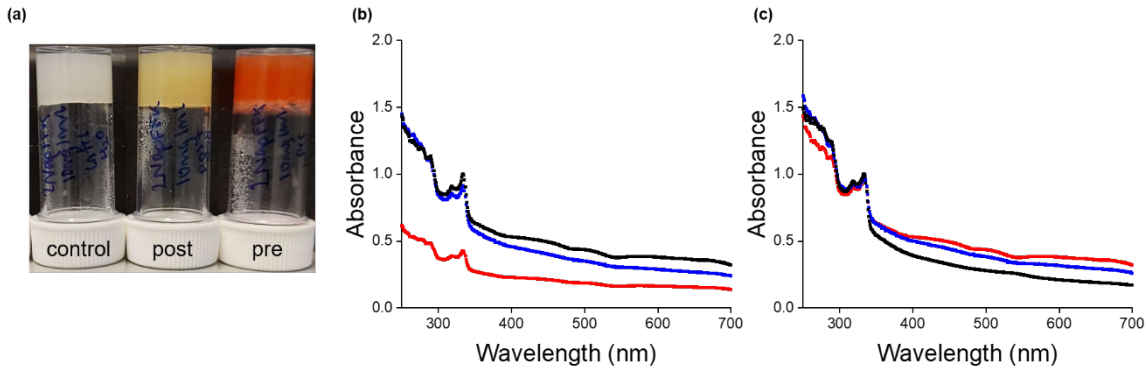

Figure S27. (a) Photographs of the gels formed from 2NapFFK at a concentration of 10 mg/mL used to collect the UV-Vis spectra, **(b)** UV-Vis spectrum showing the control sample in red, the post-gelation sample in blue and the pre-gelation sample in black, and **(c)** the UV-Vis spectrum normalised to the peak at 334 nm.

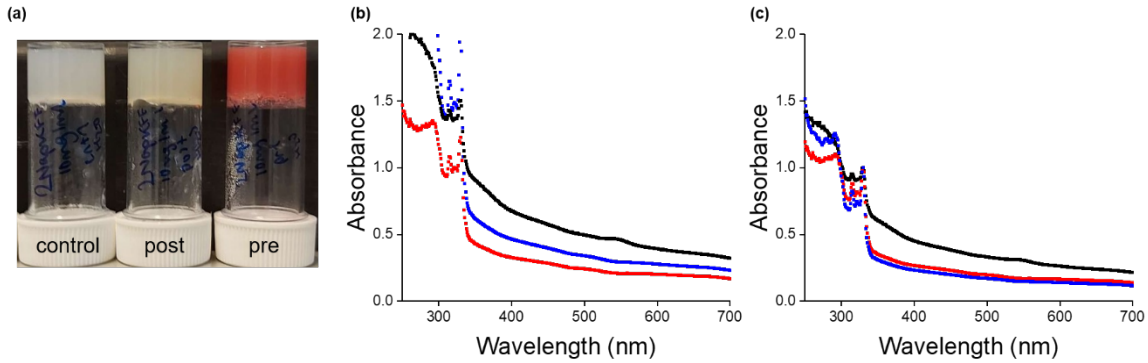

Figure S28. (a) Photographs of the gels formed from 2NapKFF at a concentration of 10 mg/mL used to collect the UV-Vis spectra, **(b)** UV-Vis spectrum showing the control sample in red, the post-gelation sample in blue and the pre-gelation sample in black, and **(c)** the UV-Vis spectrum normalised to the peak at 330 nm.

7. Characterisation of 2NapFF at each stage of synthesis

Boc-FF-OMe

(a)

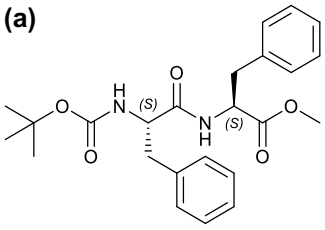

(b)

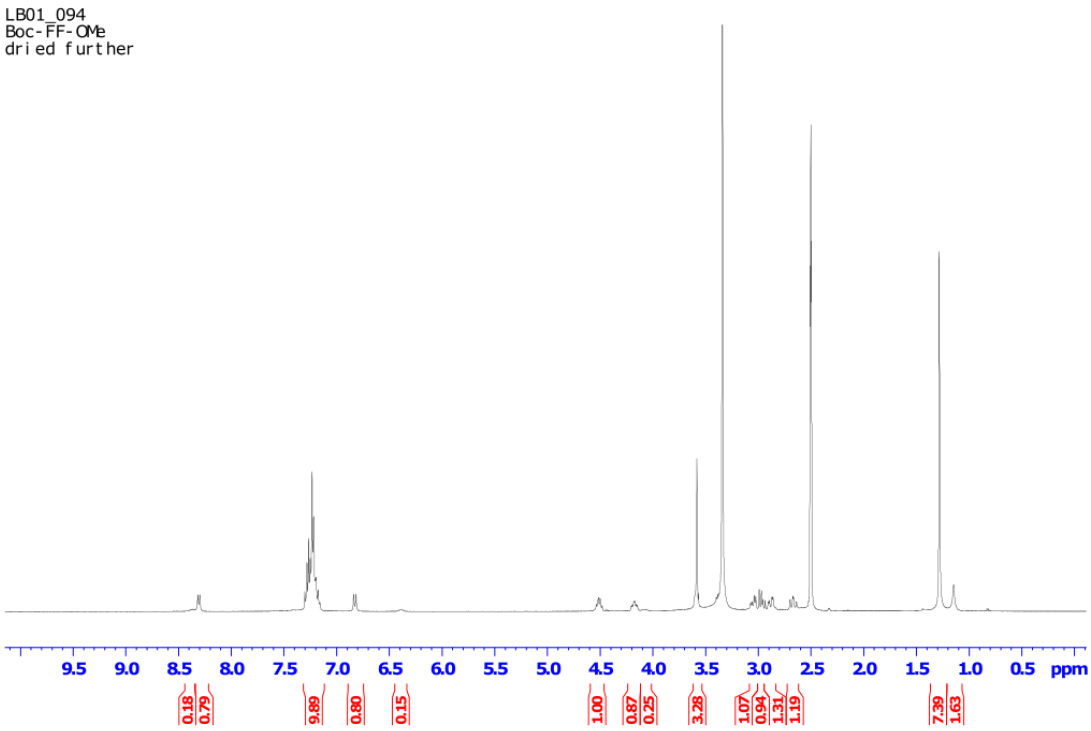

Figure S29. (a) Chemical structure of Boc-FF-OMe, product of the coupling reaction between Boc-F and HCl.F-OMe, (b) ^{1}H NMR of Boc-FF-OMe in *d*$_6$-DMSO at 25°C.

δ_H(400 MHz, DMSO$_{d6}$): 8.38 (0.2H, d, *J* = 7.8 Hz, NH), 8.31 (0.8H, d, *J* = 7.6 Hz, NH), 7.30-7.16 (10H, m, ArH), 6.83 (0.8H, d, *J* = 8.9 Hz, NH), 6.39 (0.2H, d, *J* = 8.5 Hz, NH), 4.53-4.48 (1H, m, *CH), 4.20-4.15 (0.8H, m, *CH), 4.10-4.04 (0.2H, m, *CH), 3.58 (3H, s, $COOCH_3$), 3.34 (s, H_2O), 3.05 (1H, dd, *J* = 13.8, 5.7 Hz, CH_2), 2.96 (1H, dd, *J* = 13.8, 8.6 Hz, CH_2), 2.88 (1H, dd, *J* = 13.7, 4.0 Hz, CH_2), 2.67 (1H, dd, *J* = 13.1, 10.8 Hz, CH_2), 2.50 (quintet, *d*$_6$-DMSO), 1.28 (7.4H, s, $(CH_3)_3$), 1.14 (1.6H, s, $(CH_3)_3$).

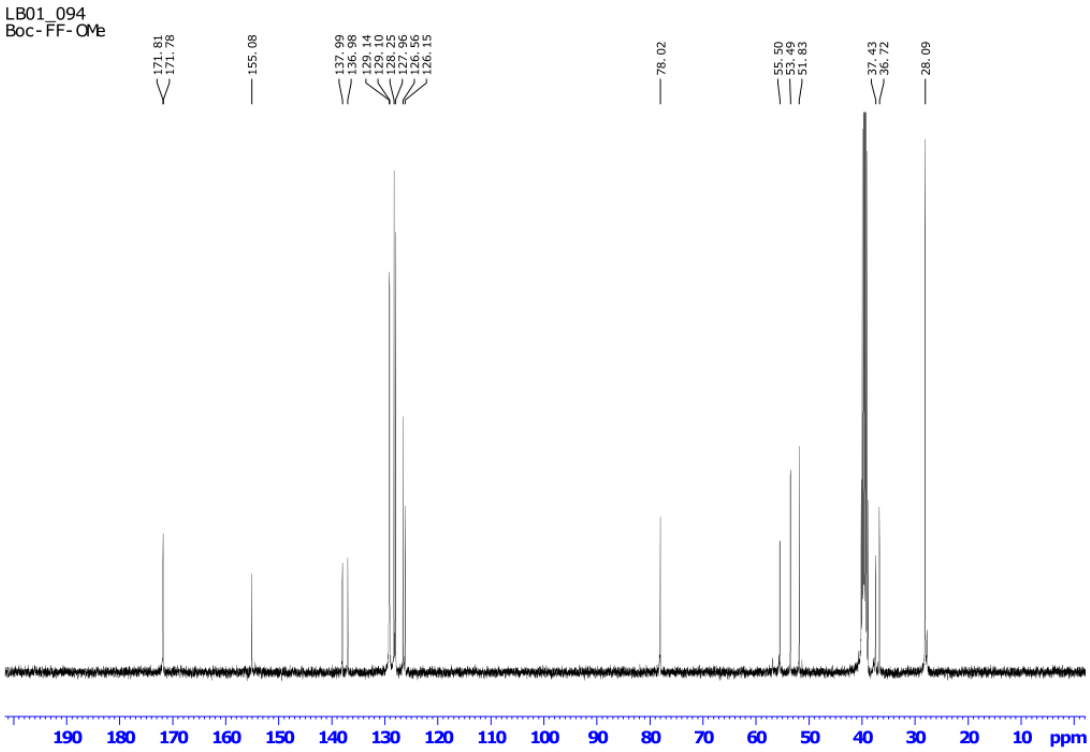

Figure S30. ^{13}C NMR of Boc-FF-OMe in d_6-DMSO at 25°C.

δ_{13C}(100 MHz, DMSO$_{d6}$): 171.81 (C=O), 171.78 (C=O), 155.08 (C=O), 137.99 (ArC), 136.98 (ArC), 129.14 (ArC), 129.10 (ArC), 128.25 (ArC), 127.96 (ArC), 126.56 (ArC), 126.15 (ArC), 78.02 (**C**(CH_3), 55.50 (*CH), 53.49 (*CH), 51.83 (COO**C**H_3), 39.50 (septet, d_6-DMSO), 37.43 (CH_2Ph), 36.72 (CH_2Ph)), 28.09 (C(**C**H_3)$_3$.

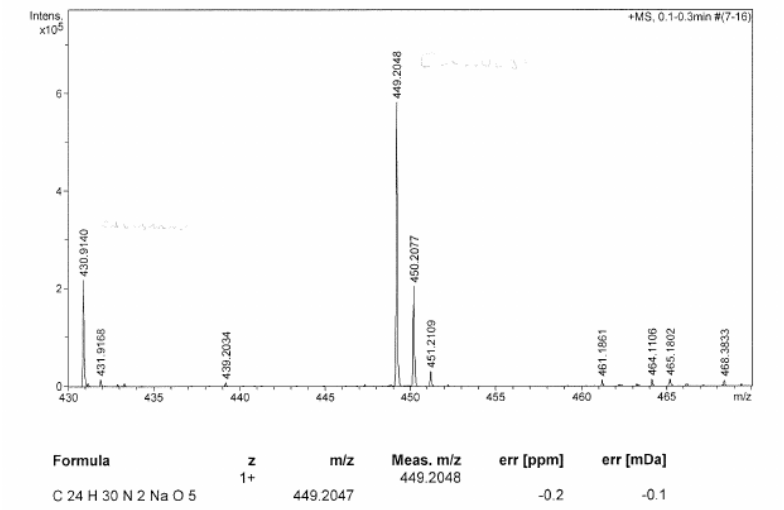

Figure S31. Mass spectrum of Boc-FF-OMe. **HRMS (ESI) m/z: ([M$^+$Na]$^+$).** Accurate Mass calculated for $C_{24}H_{30}N_2NaO_5$: 449.2047. Found: 449.2048.

TFA.FF-OMe

(a)

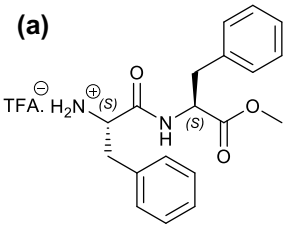

(b)

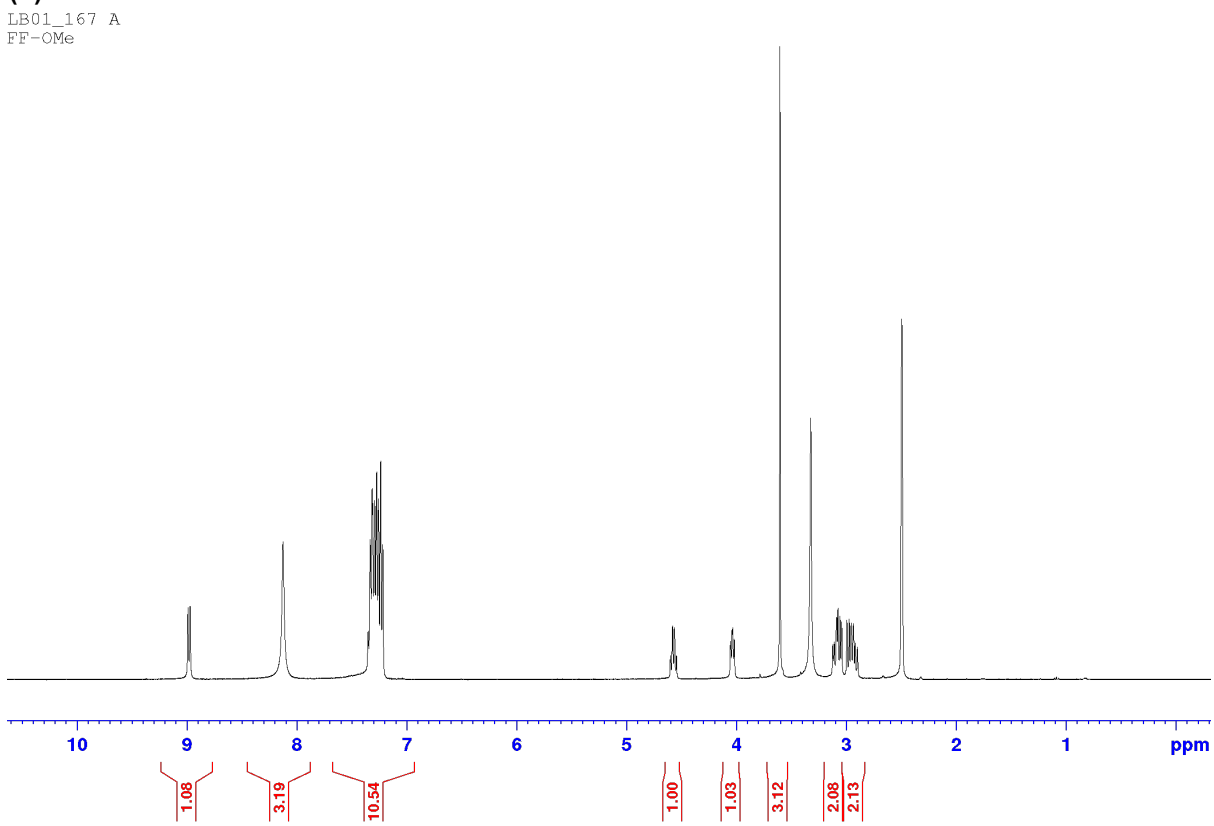

Figure 32. (a) Chemical structure of TFA.FF-OMe, product of Boc-deprotection of Boc-FF-OMe, (b) ^{1}H NMR of TFA.FF-OMe in d_6-DMSO at 25°C. The baseline of the spectrum has been expanded to the range 10-0 ppm.

δ_H(400 MHz, DMSO$_{d6}$): 8.98 (1H, d, J = 7.6 Hz, NH), 8.12 (3H, s, NH_3^+), 7.35-7.22 (10H, m, ArH), 4.60-4.55 (1H, m, *CH), 4.06-4.02 (1H, m, *CH), 3.61 (3H, s, $COOCH_3$), 3.33 (s, H_2O), 3.13-3.05 (2H, m, CH_2Ph), 3.00-2.90 (2H, m, CH_2Ph), 2.50 (quintet, d_6-DMSO).

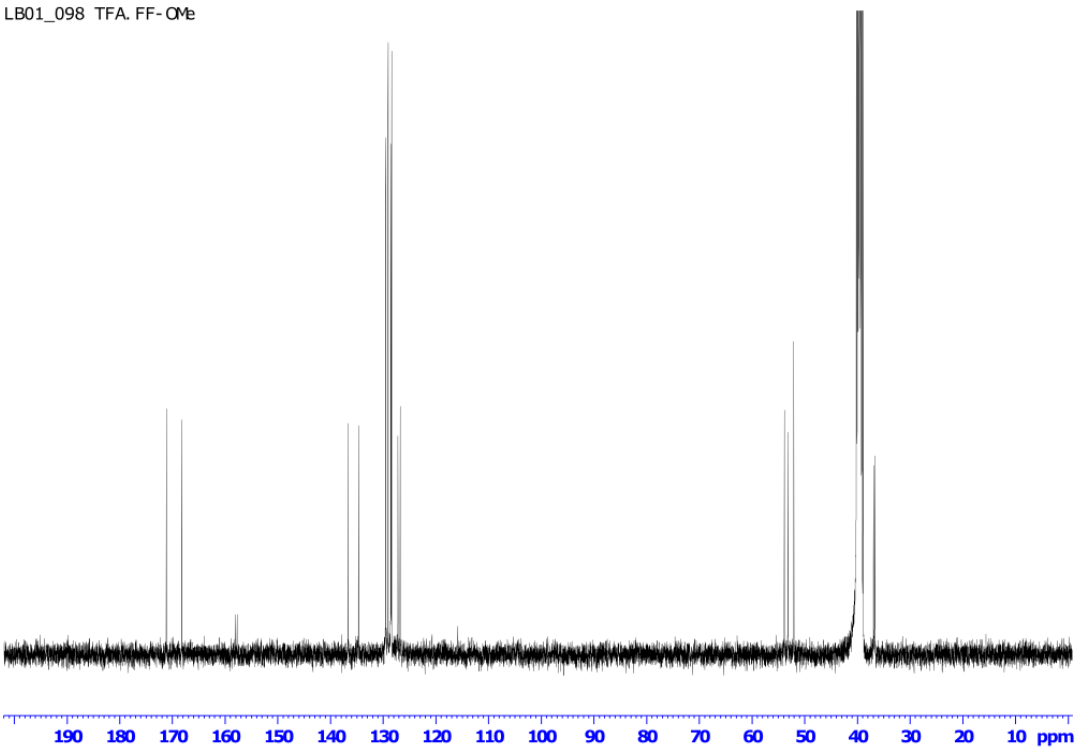

Figure S33. ^{13}C NMR of TFA.FF-OMe in d_6-DMSO at 25°C.

δ_{13C}(100 MHz, DMSO$_{d6}$): 171.13 (C=O), 168.23 (C=O), 136.64 (ArC), 134.64 (ArC), 129.50 (ArC), 129.05 (ArC), 128.52 (ArC), 128.39 (ArC), 127.18 (ArC), 126.75 (ArC), 53.81 (*CH), 53.13 (*CH), 52.03 (COO**C**H$_3$), 39.50 (septet, d_6-DMSO), 36.87 (CH_2Ph), 36.65 (CH_2Ph).

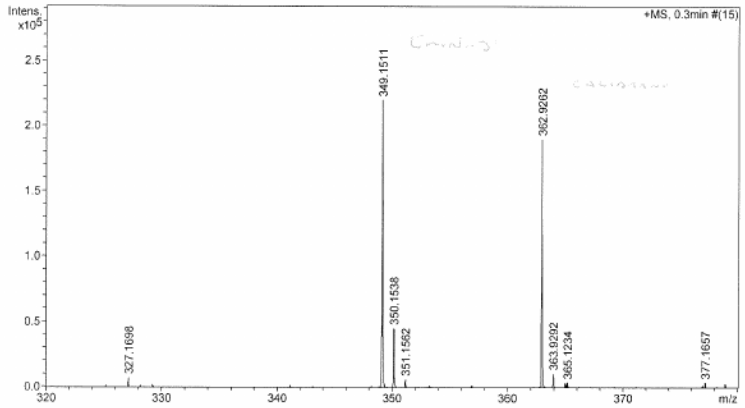

Formula	z	m/z	Meas. m/z	err [ppm]	err [mDa]
	1+		349.1511		
C 19 H 22 N 2 Na O 3		349.1523		3.4	1.2

Figure S34. Mass spectrum of TFA.FF-OMe. **HRMS (ESI) m/z: ([M$^+$Na]$^+$).** Accurate Mass calculated for $C_{19}H_{22}N_2NaO_3$: 349.1523. Found: 349.1511.

2NapFF-OMe

(a)

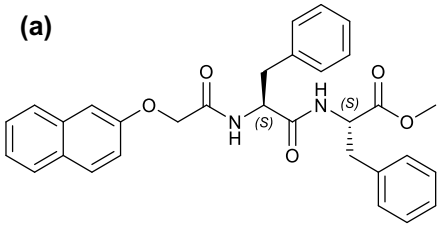

(b)

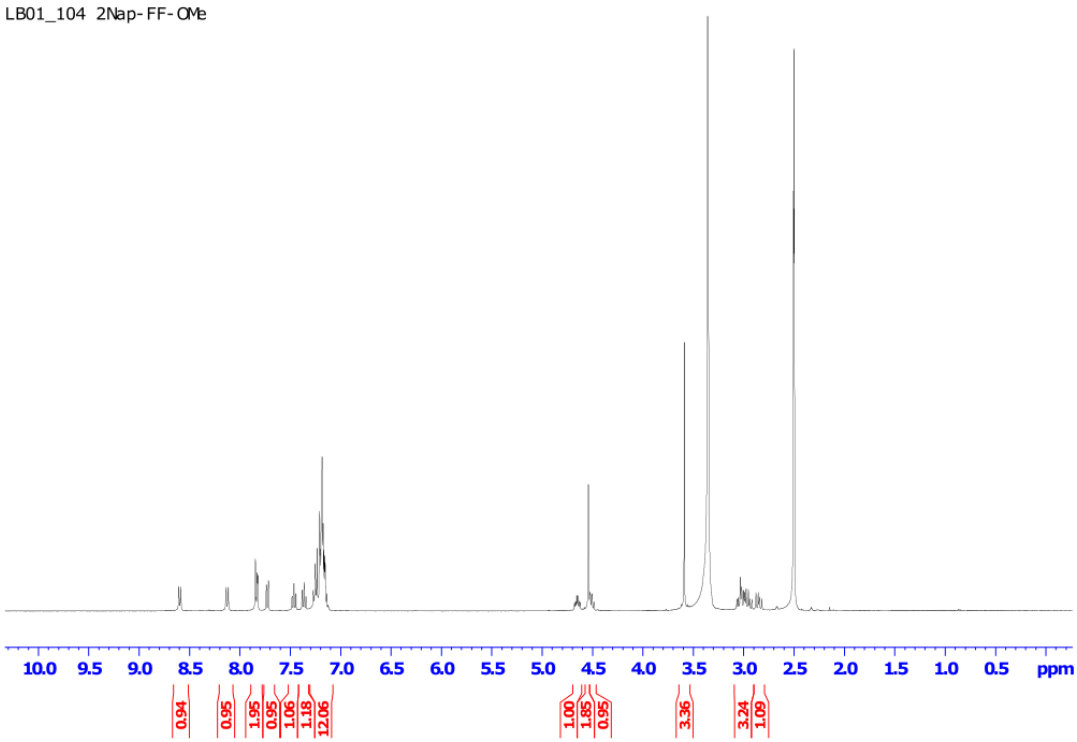

Figure S35. (a) Chemical structure of 2NapFF-OMe, the product of the coupling reaction between 2-naphthoxyacetic acid and TFA.FF-OMe, (b) ^{1}H NMR of 2NapFF-OMe in d_6-DMSO at 25°C.

δ_H(400 MHz, DMSO$_{d6}$): 8.60 (1H, d, J = 7.6 Hz, NH), 8.13 (1H, d, J = 8.5 Hz, NH), 7.85-7.82 (2H, m, ArH), 7.74-7.72 (1H, m, ArH), 7.47-7.44 (1H, m, ArH), 7.38-7.34 (1H, m, ArH), 7.27-7.12 (12H, m, ArH), 4.68-4.62 (1H, m, *CH), 4.54 (2H, s, 2Nap-OC**H**$_2$), 4.52-4.49 (1H, m, *CH), 3.36 (3H, s, COOC**H**$_3$), 3.07-2.92 (3H, m, *CHC**H**$_2$), 2.85 (1H, dd, J = 13.8, 9.5, *CHC**H**$_2$), 2.50 (quintet d_6-DMSO).

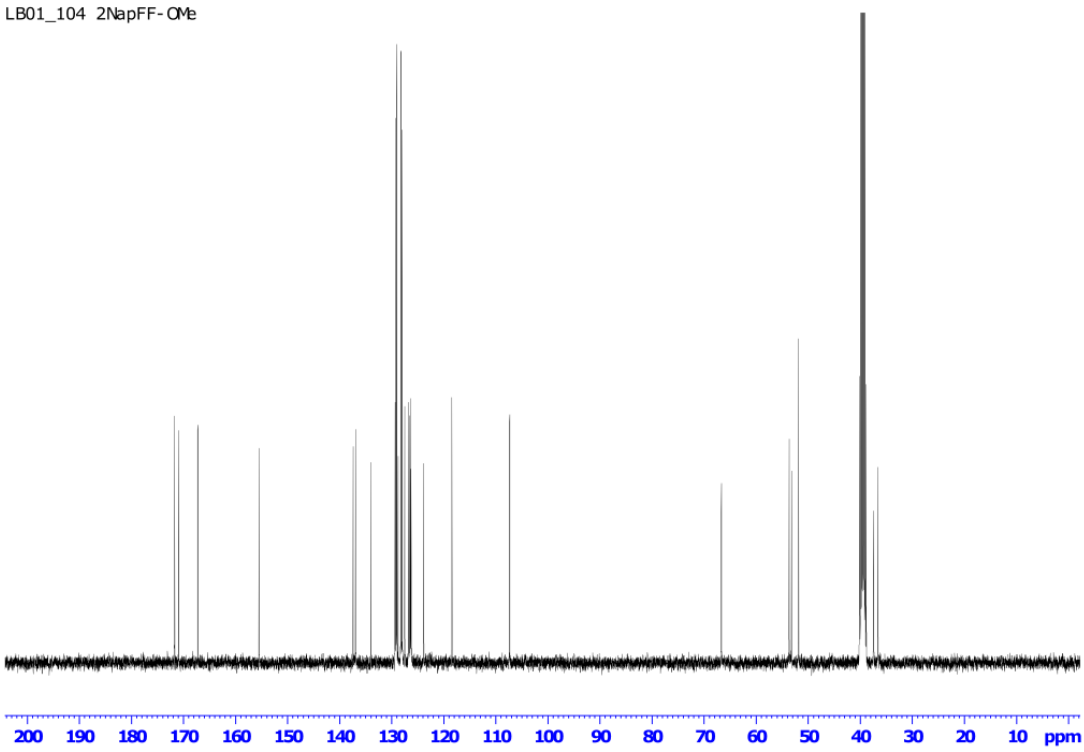

Figure S36. ^{13}C NMR of 2NapFF-OMe in *d*$_6$-DMSO at 25°C.

δ_{13C}(100 MHz, DMSO$_{d6}$): 171.70 (C=O), 170.95 (C=O), 167.26 (C=O), 155.49 (ArC), 137.41 (ArC), 136.94 (ArC), 134.03 (ArC), 129.36 (ArC), 129.20 (ArC), 129.05 (ArC), 128.75 (ArC), 128.26 (ArC), 128.00 (ArC), 127.50 (ArC), 126.78 (ArC), 126.58 (ArC), 126.43 (ArC), 126.29 (ArC), 123.87 (ArC), 118.45 (ArC), 107.34 (ArC), 66.68 (2Nap-OCH_2), 53.65 (*CH), 53.19 (*CH), 51.86 (COO**C**H_3), 39.50 (septet, *d*$_6$-DMSO), 37.43 (CH_2), 36.63 (CH_2).

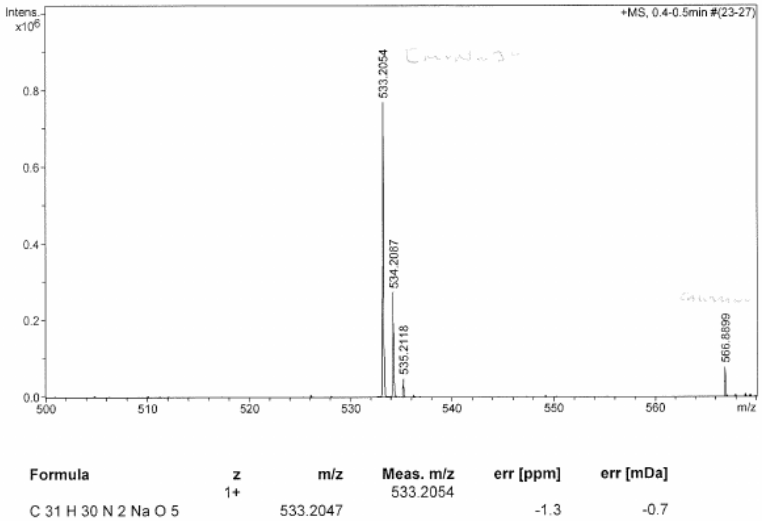

Figure S37. Mass spectrum of 2NapFF-OMe. **HRMS (ESI) m/z: ([M$^+$Na]$^+$).** Accurate Mass calculated for $C_{31}H_{30}N_2NaO_5$: 533.2047. Found: 533.2054.

2NapFF

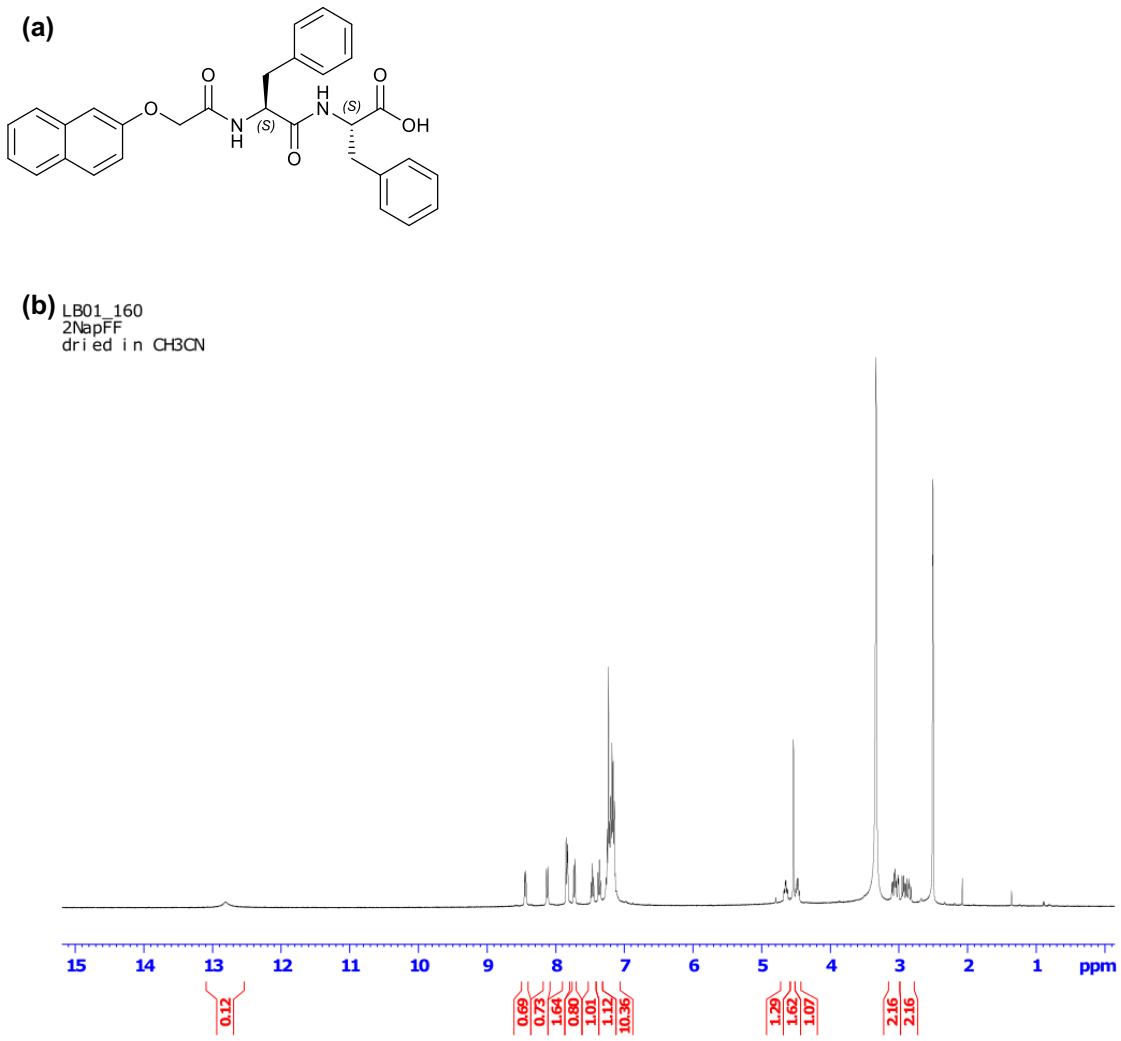

Figure S38. (a) chemical structure of 2NapFF, product of methyl ester deprotection of 2NapFF-OMe, (b) ^{1}H NMR of 2NapFF in d_6-DMSO at 25°C.

δ_H(400 MHz, DMSO$_{d6}$): 12.81 (1H, s, COOH), 8.44 (1H, d, J = 7.9 Hz, NH), 8.12 (1H, d, J 8.4, NH), 7.85-7.82 (2H, m, ArH), 7.74-7.72 (1H, m, ArH), 7.48-7.45 (1H, m, ArH), 7.38-7.34 (1H, m, ArH), 7.27-7.11 (12H, m, ArH), 4.67-4.62 (1H, m, *CH), 4.53 (2H, s, 2Nap-OCH$_2$), 4.50-4.45 (1H, m, *CH), 3.33 (s, H$_2$O), 3.10-3.00 (2H, m, *CHC**H$_2$**), 2.95-2.82 (2H, m, *CHC**H$_2$**), 2.50 (quintet, d_6-DMSO), 2.07 (s, CH$_3$CN).

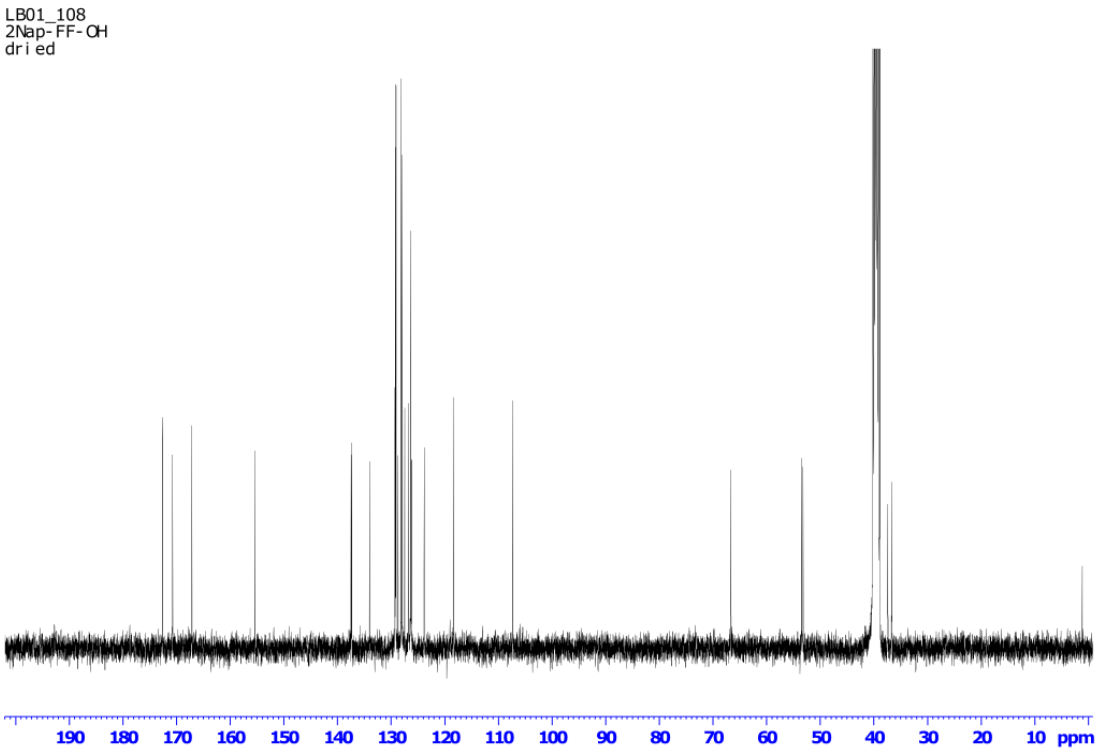

Figure S39. ^{13}C NMR of 2NapFF in *d*$_6$-DMSO at 25°C.

δ$_{13C}$(100 MHz, DMSO$_{d6}$): 172.64 (C=O), 170.74 (C=O), 167.15 (C=O), 155.45 (ArC), 137.46 (ArC), 137.34 (ArC), 133.98 (ArC), 129.30 (ArC), 129.19 (ArC), 129.08 (ArC), 128.70 (ArC), 128.12 (ArC), 127.92 (ArC), 127.45 (ArC), 126.74 (ArC), 126.38 (ArC), 126.19 (ArC), 123.81 (ArC), 118.39 (ArC), 107.31 (ArC), 66.65 (2Nap-O**C**H$_2$), 53.47 (*CH), 53.18 (*CH), 39.50 (septet, *d*$_6$-DMSO), 37.37 (*CH**C**H$_2$), 36.65 (*CH**C**H$_2$).

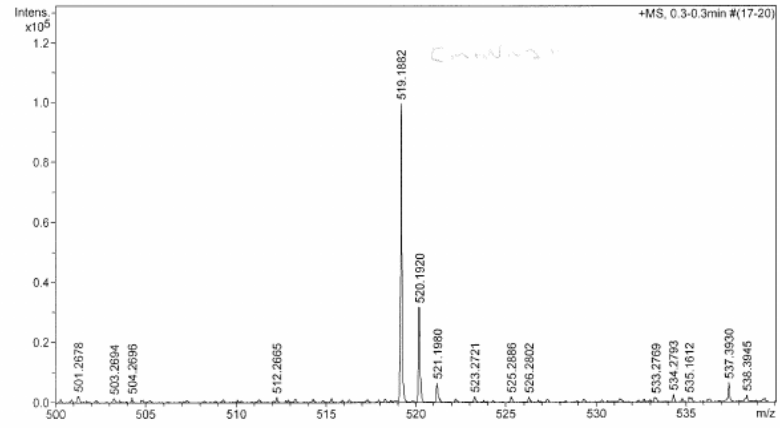

Formula	z	m/z	Meas. m/z	err [ppm]	err [mDa]
	1+		519.1882		
C 30 H 28 N 2 Na O 5		519.1890		1.7	0.9

FigureS40. Mass spectrum of 2NapFF. **HRMS (ESI) m/z: ([M$^+$Na]$^+$).** Accurate Mass calculated for $C_{30}H_{28}N_2NaO_5$: 519.1890. Found: 519.1882.

8. Characterisation of 2NapFFK at each stage of synthesis following synthesis of 2NapFF

2NapFFK(Boc)-OMe

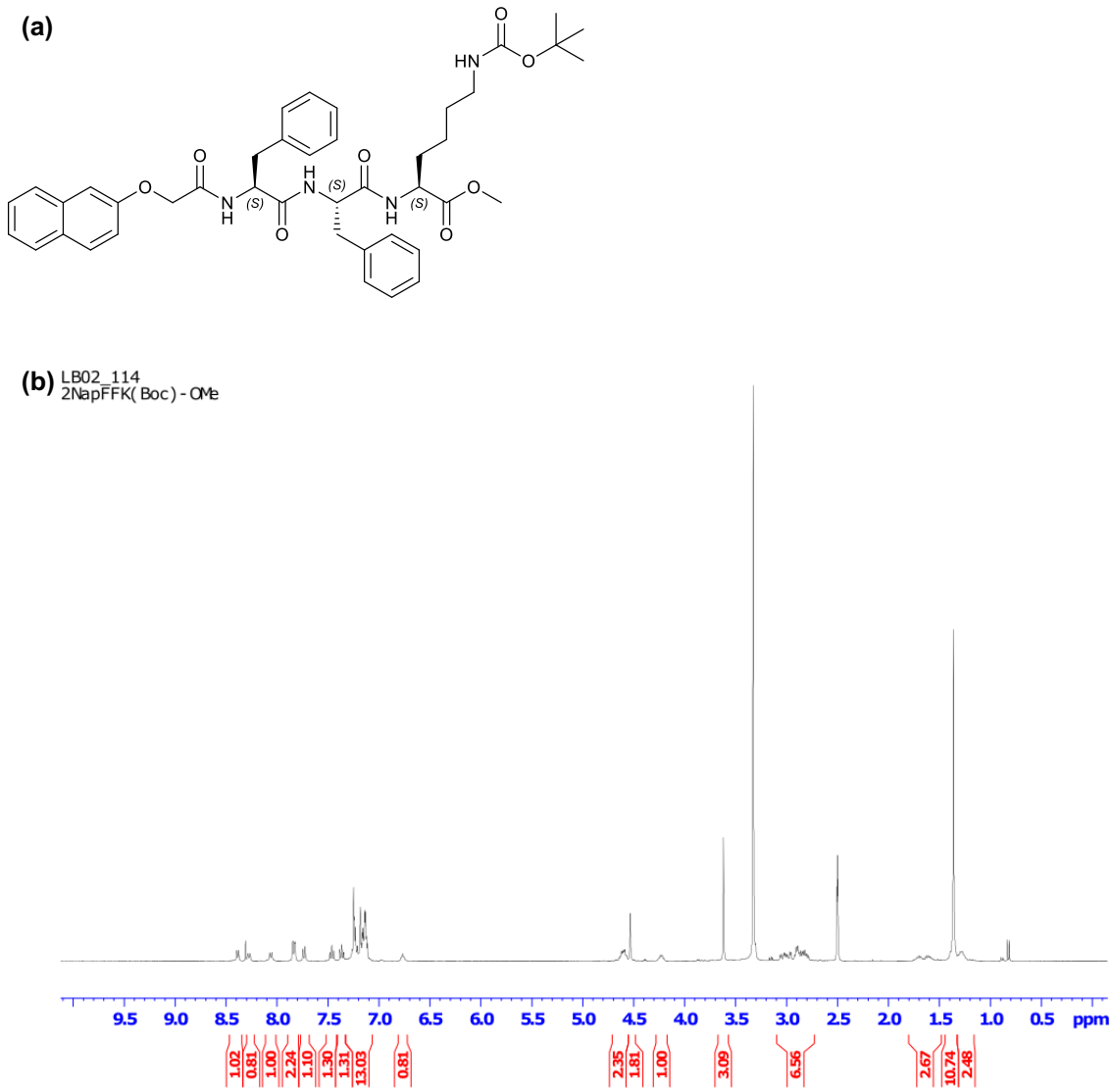

Figure S41. (a) Chemical structure of 2NapFFK(Boc)-OMe, the product of the coupling reaction between 2NapFF and HCl.K(Boc)-OMe, (b) ^{1}H NMR of 2NapFFK(Boc)-OMe in d_6-DMSO at 25°C.

δ_H(400 MHz, DMSO$_{d6}$): 8.39 (1H, d, J = 7.3 Hz, NH), 8.31 (s, CH_3Cl), 8.27 (1H, d, J = 7.9 Hz, NH), 8.06 (01H, d, J = 8.1 Hz, NH), 7.85-7.82 (2H, m, ArH), 7.75-7.73 (1H, m, ArH), 7.48-7.44 (1H, m, ArH), 7.38-7.34 (1H, m, ArH), 7.26-7.11 (12H, m, ArH), 6.78-6.75 (1H, m, NH-Boc), 4.64-4.56 (2H, m, *CH), 4.53 (2H, s, 2Nap-OCH_2), 4.26-4.20 (2H, m, *CH), 3.62 (3H, s, $COOCH_3$), 3.32 (s, H_2O), 3.06-2.78 (6H, m, CH_2), 2.50 (quintet, d_6-DMSO), 1.75-1.55 (2.5H, m, CH_2), 1.36-1.35 (9H, m, $C(CH_3)_3$), 1.32-1.21 (2.5H, m, CH_2).

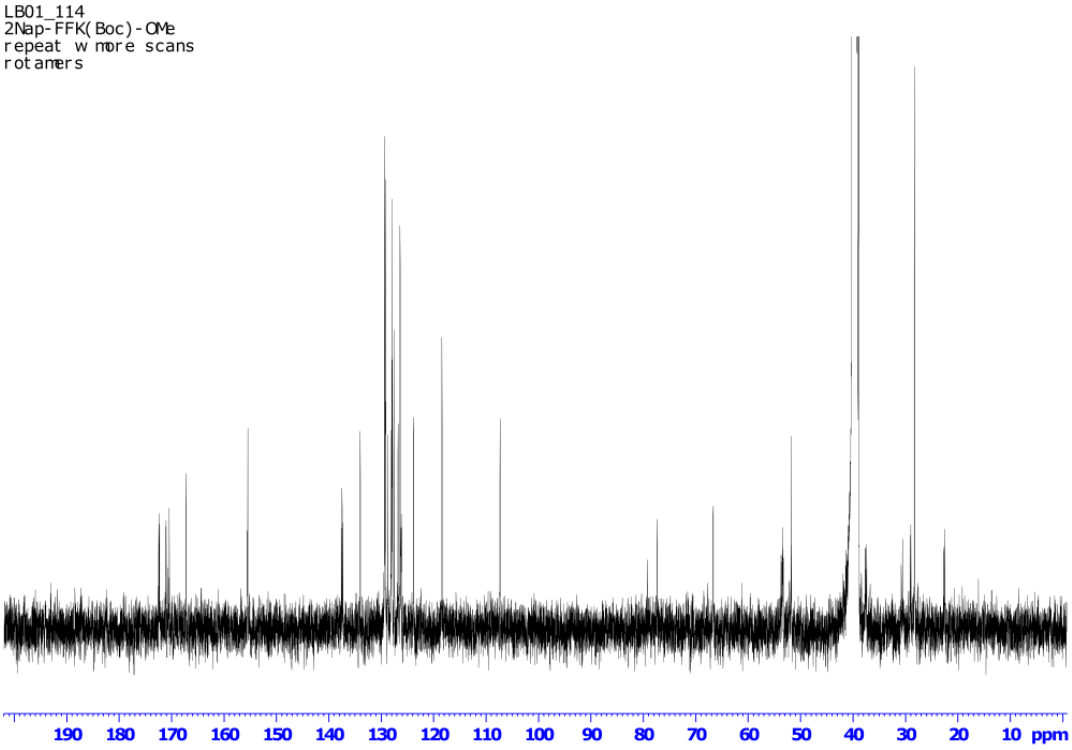

Figure S42. ^{13}C NMR of 2NapFFK(Boc)-OMe in d_6-DMSO at 25°C.

δ_{13C}(100 MHz, DMSO$_{d6}$): 172.43 (C=O), 172.30 (C=O), 171.07 (C=O), 171.02 (C=O), 170.42 (C=O), 167.18 (C=O), 155.53 (C=O), 155.44 (ArC), 137.60 (ArC), 137.48 (ArC), 137.42 (ArC), 137.34 (ArC), 133.99 (ArC), 129.32 (ArC), 129.19 (ArC), 129.16 (ArC), 129.11 (ArC), 128.73 (ArC), 128.71 (ArC), 128.11 (ArC), 127.98 (ArC), 127.93 (ArC), 127.90 (ArC), 127.83 (ArC), 127.46 (ArC), 126.76 (ArC), 126.38 (ArC), 123.82 (ArC), 118.39 (ArC), 107.33 (ArC), 107.30 (ArC), 77.31 (**C**$(CH_3)_3$), 77.29 (**C**$(CH_3)_3$), 66.65 (2Nap-OCH_2), 66.62 (2Nap-OCH_2), 53.69 (*CH), 53.56 (*CH), 53.49 (*CH), 53.42 (*CH), 53.34 (*CH), 53.23 (*CH), 51.80 (COO**C**H_3), 51.70 (COO**C**H_3), 39.50 (septet, d_6-DMSO), 37.61 (CH_2), 37.36 (CH_2), 30.76 (CH_2), 30.52 (CH_2), 29.06 (CH_2), 28.91 (CH_2), 28.22 (C(**C**$H_3)_3$), 22.60 (CH_2), 22.43 (CH_2).

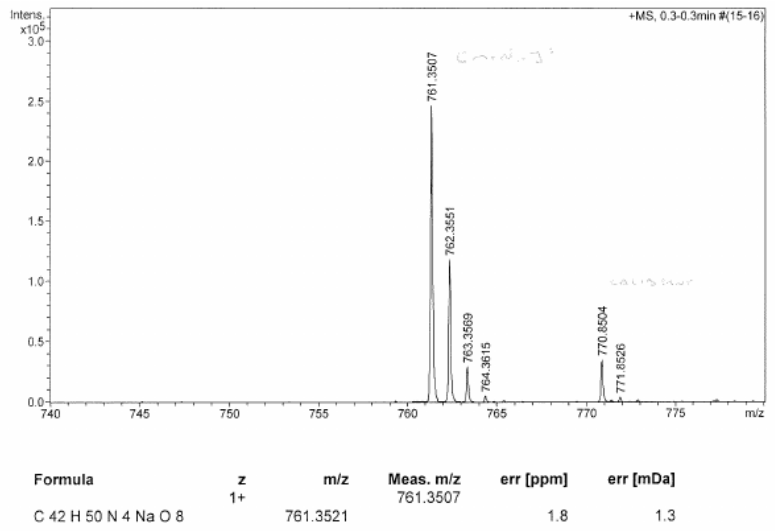

Figure 43. Mass spectrum of 2NapFFK(Boc)-OMe. **HRMS (ESI) m/z: ([M$^+$Na]$^+$).** Accurate Mass calculated for $C_{42}H_{50}N_4NaO_8$: 761.3521. Found: 761.3507

2NapFFK(Boc)

(a)

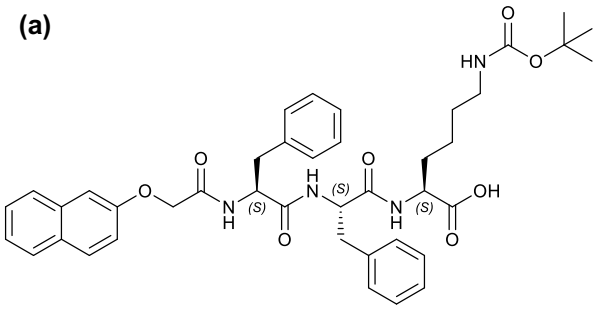

(b) LB02_118
2NapFFK(Boc)

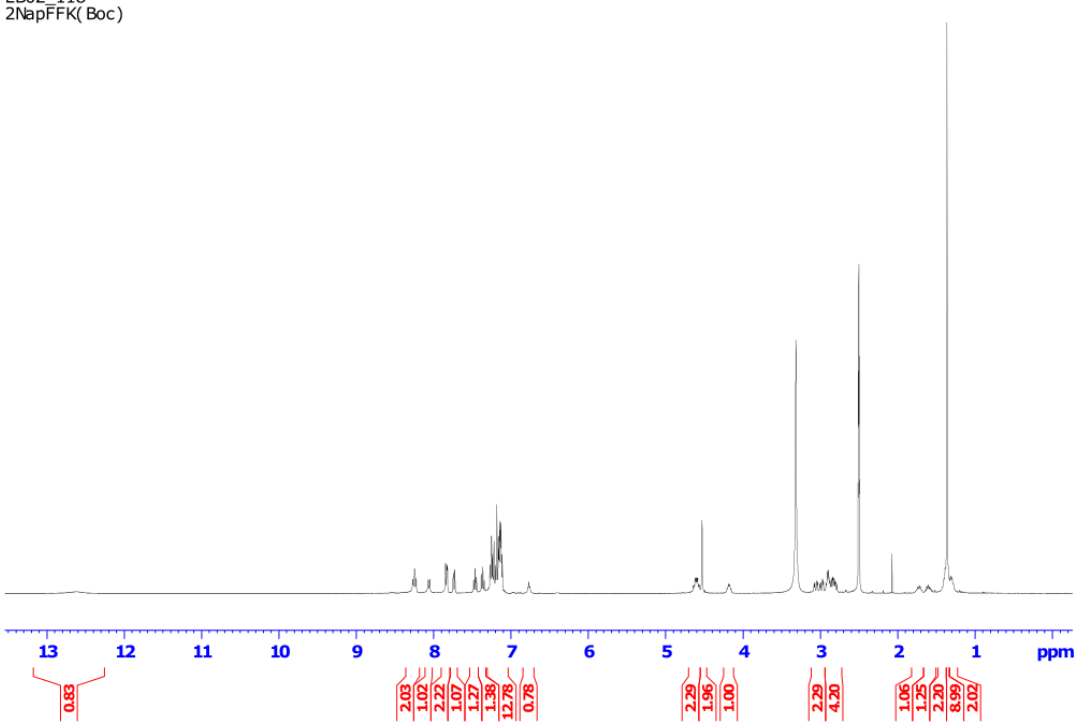

Figure S44. (a) Chemical structure of 2NapFFK(Boc), product of methyl ester deprotection of 2NapFFK(Boc)-OMe, (b) ^{1}H NMR of 2NapFFK(Boc) in d_6-DMSO at 25°C.

δ_H(400 MHz, DMSO$_{d6}$): 12.62 (1H, s, COOH), 8.26 (1H, d, J = 9.2 Hz, NH), 8.24 (1H, d, J = 8.1 Hz, NH), 8.06 (1H, d, J = 8.4 Hz, NH), 7.84-7.82 (2H, m, ArH), 7.75-7.72 (1H, m, ArH), 7.48-7.44 (1H, m, ArH), 7.38-7.34 (1H, m, ArH), 7.27-7.10 (12H, m, ArH), 6.97-6.95 (0.6H, m, ArH), 6.78-6.75 (1H, m, NH-Boc), 4.64-4.56 (2H, m, *CH), 4.53 (2H, s, 2Nap-OCH$_2$), 4.20-4.15 (1H, m, *CH), 3.31 (s, H$_2$O), 3.06 (1H, dd, J = 14.0, 4.3 Hz, CH$_2$), 2.98 (1H, dd J = 13.9, 4.2 Hz, CH$_2$), 2.92-2.78 (4H, m, CH$_2$), 2.50 (quintet, d_6-DMSO), 2.07 (s, CH$_3$CN), 1.77-1.69 (1H, m, CH$_2$), 1.55-1.42 (1H, m, CH$_2$), 1.42-1.23 (4H, m, CH$_2$) 1.36 (9H, s, C(CH$_3$)$_3$).

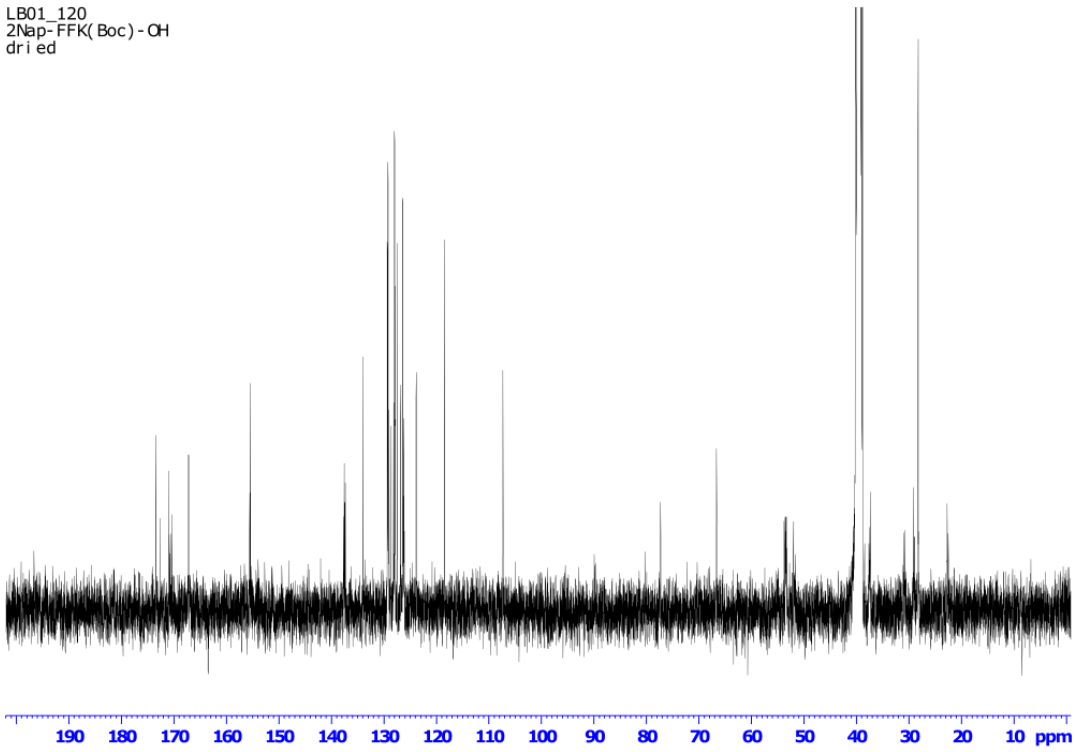

Figure S45. ^{13}C NMR of 2NapFFK(Boc) in d_6-DMSO at 25°C.

δ_{13C}(100 MHz, DMSO$_{d6}$): 173.39 (C=O), 172.66 (C=O), 170.94 (C=O), 170.86 (C=O), 170.49 (C=O), 170.39 (C=O), 167.19 (C=O), 167.16 (C=O), 155.54 (C=O), 155.43 (ArC), 137.68 (ArC), 137.56 (ArC), 137.44 (ArC), 137.35 (ArC), 134.00 (ArC), 129.34 (ArC), 129.23 (ArC), 129.17 (ArC), 129.09 (ArC), 128.73 (ArC), 128.72 (ArC), 128.14 (ArC), 127.97 (ArC), 127.90 (ArC), 127.83 (ArC), 127.47 (ArC), 126.79 (ArC), 126.76 (ArC), 126.39 (ArC), 126.33 (ArC), 126.22 (ArC), 126.18 (ArC), 123.84 (ArC), 118.40 (ArC), 107.33 (ArC), 107.32 (ArC), 77.33 (**C**(CH$_3$)$_3$), 66.67 (2Nap-OCH$_2$), 53.76 (*CH), 53.54 (*CH), 53.49 (*CH), 53.41 (*CH), 53.34 (*CH), 53.21 (*CH), 51.97 (*CH), 51.95 (*CH), 39.50 (septet, d_6-DMSO), 30.96 (CH$_2$), 30.78 (CH$_2$), 29.12 (CH$_2$), 28.97 (CH$_2$), 28.24 (C(**C**H$_3$)$_3$), 22.72 (CH$_2$), 22.50 (CH$_2$).

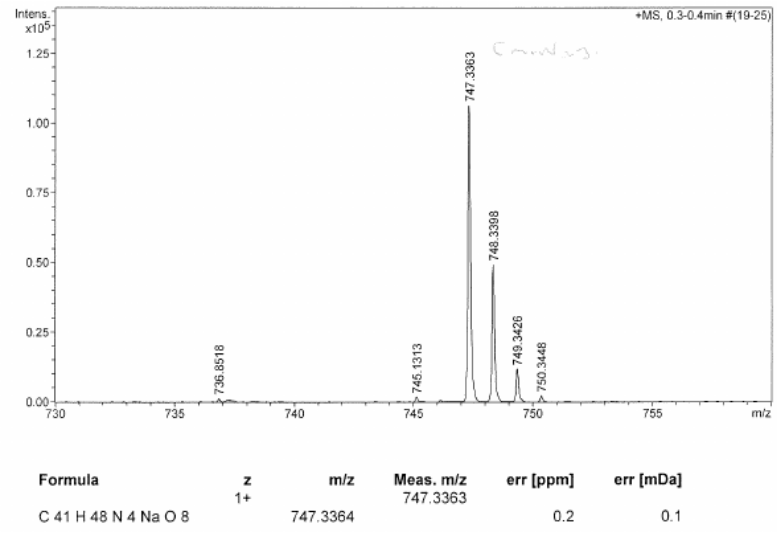

Formula	z	m/z	Meas. m/z	err [ppm]	err [mDa]
	1+		747.3363		
C 41 H 48 N 4 Na O 8		747.3364		0.2	0.1

Figure S46. Mass spectrum of 2NapFFK(Boc). **HRMS (ESI) m/z: ([M$^+$Na]$^+$).** Accurate Mass calculated for $C_{41}H_{48}N_4NaO_8$: 747.3364. Found: 747.3363

2NapFFK

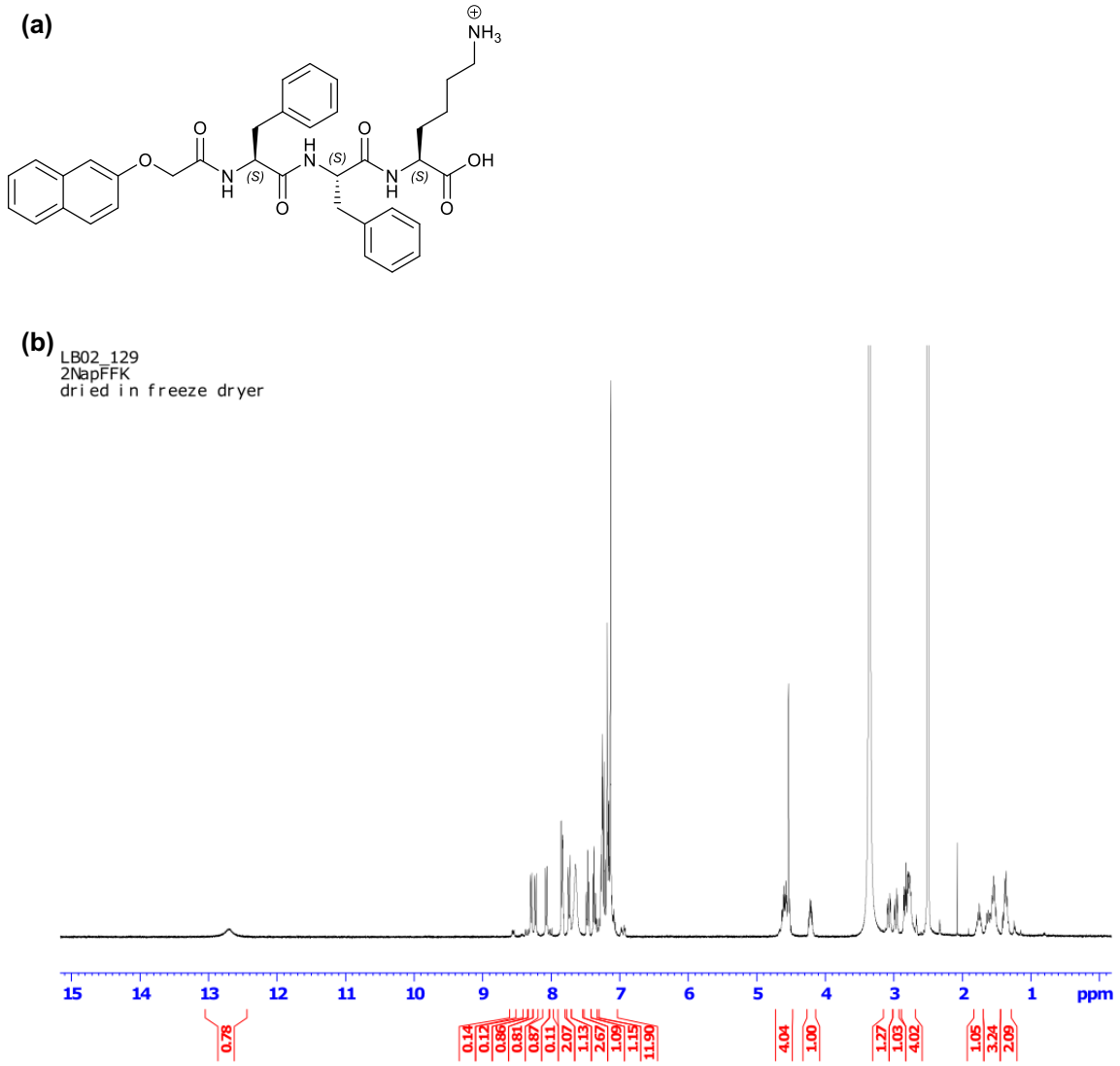

Figure S47. (a) Chemical structure of 2NapFFK, product of Boc deprotection of 2NapFFK(Boc), (b) ^{1}H NMR of 2NapFFK in d_6-DMSO at 25°C.

δ_H(400 MHz, DMSO$_{d6}$): 12.71 (1H, s, COOH), 8.29 (1H, d, J = 7.9 Hz, NH), 8.23 (1H, d, J = 8.4 Hz, NH), 8.07 (1H, d, J = 8.4 Hz, NH), 7.85-7.83 (2, m, ArH), 7.75-7.72 (1H, m, ArH), 7.64 (3H, s, NH_3^+), 7.49-7.45 (1H, m, ArH), 7.39-7.35 (1H, m, ArH), 7.28-7.06 (12H, m, ArH), 4.63-4.49 (2H, m, *CH), 4.53 (2H, s, 2Nap-OCH_2), 4.24-4.19 (1H, m, *CH), 3.35 (s, H_2O), 3.07 (1H, dd, J = 13.7, 4.1 Hz, CH_2), 2.97 (2H, dd, J = 14.2, 4.5 Hz, CH_2), 2.85-2.75 (4H, m, CH_2), 2.50 (quintet, d_6-DMSO), 2.07 (s, CH_3CN), 1.81-1.72 (1H, m, CH_2), 1.66-1.51 (3H, m, CH_2), 1.41-1.32 (2H, m, CH_2), purity: 99%.

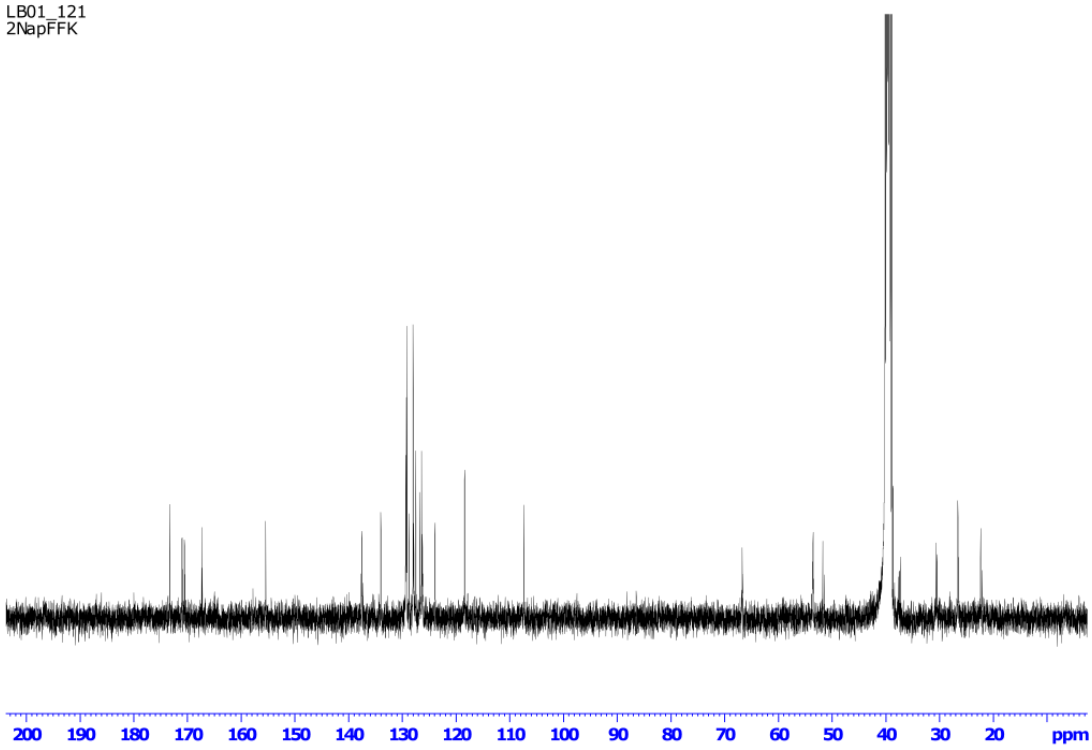

Figure S48. ^{13}C NMR of 2NapFFK in d_6-DMSO at 25°C.

δ_{13C}(100 MHz, DMSO$_{d6}$): 173.30 (C=O), 173.28 (C=O), 171.01 (C=O), 170.94 (C=O), 170.56 (C=O), 170.48 (C=O), 167.33 (C=O), 167.25 (C=O), 155.45 (ArC), 155.43 (ArC), 137.69 (ArC), 137.53 (ArC), 137.48 (ArC), 137.34 (ArC), 136.34 (ArC), 134.01 (ArC), 129.38 (ArC), 129.35 (ArC), 129.25 (ArC), 129.16 (ArC), 128.76 (ArC), 128.74 (ArC), 128.01 (ArC), 127.96 (ArC), 127.87 (ArC), 127.49 (ArC),126.81 (ArC), 126.77 (ArC), 126.44 (ArC), 126.27 (ArC), 126.22 (ArC), 123.90 (ArC), 123.87 (ArC), 118.40 (ArC), 107.37 (ArC), 107.34 (ArC), 66.71 (2Nap-OCH_2), 66.66 (2Nap-OCH_2), 53.59 (*CH), 53.53 (*CH), 53.49 (*CH), 53.47 (*CH), 51.71 (*CH), 51.46 (*CH), 39.50 (septet, d_6-DMSO), 38.64 (CH_2), 38.61 (CH_2), 30.67 (CH_2), 30.46 (CH_2), 26.56 (CH_2), 26.50 (CH_2), 22.33 (CH_2), 22.10 (CH_2).

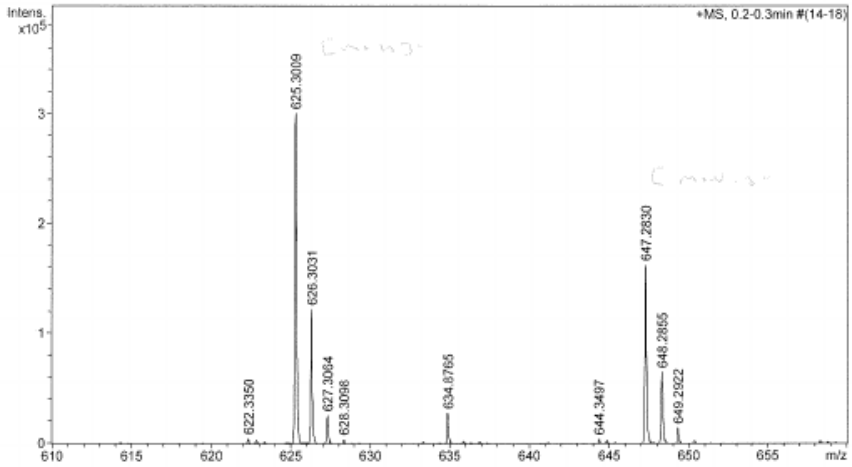

Formula	z	m/z	Meas. m/z	err [ppm]	err [mDa]
	1+		625.3009		
C 36 H 41 N 4 O 6		625.3021		1.9	1.2
	1+		647.2830		
C 36 H 40 N 4 Na O 6		647.2840		1.6	1.0

Figure S49. Mass spectrum of 2NapFFK. **HRMS (ESI) m/z: ([M$^+$Na] $^+$).** Accurate Mass calculated for $C_{36}H_{40}N_4NaO_6$: 647.2840. Found: 647.2830

9. Characterisation of 2NapKFF at each stage of synthesis.

2NapK(Boc)-OMe

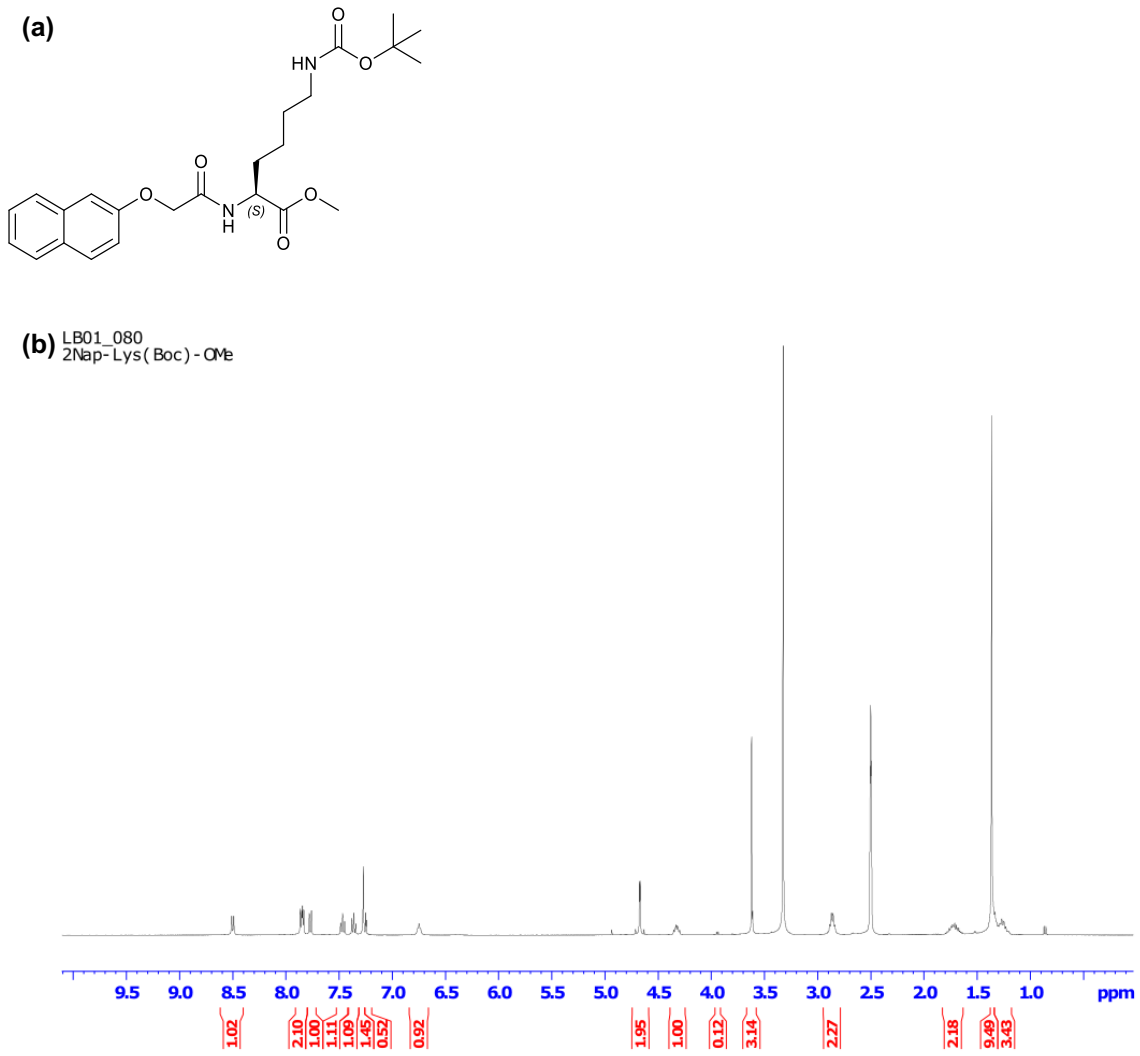

Figure S50. (a) Chemical structure of 2NapK(Boc)-OMe, product of the coupling reaction between 2-naphthoxyacetic acid and K(Boc)-OMe, (b) ^{1}H NMR of 2NapK(Boc)-OMe in d_6-DMSO at 25°C.

δ_H(400 MHz, DMSO$_{d6}$): 8.50 (1H, d, J = 7.8 Hz, NH), 7.85 (2H, dd, J = 8.3, 4.9 Hz, ArH), 7.77 (1H, d, J = 8.2 Hz, ArH), 7.47 (1H, m, ArH), 7.36 (1H, m, ArH), 7.27 (1.5H, s, ArH), 7.25-7.24 (0.5H, m, ArH), 6.76-6.73 (1H, m, NH-Boc), 4.67 (2H, dd, J = 14.7, 14.7 Hz, 2Nap-OCH$_2$), 4.35-4.30 (1H, m, *CH), 3.62 (3H, s, COOCH$_3$), 3.32 (s, H$_2$O), 2.90-2.84 (2H, m, C**H$_2$**NHBoc), 2.50 (q, d_6-DMSO), 1.80-1.64 (2H, m, CH$_2$), 1.36 (9H, s, (CH$_3$)$_3$), 1.33-1.20 (4H, m, CH$_2$).

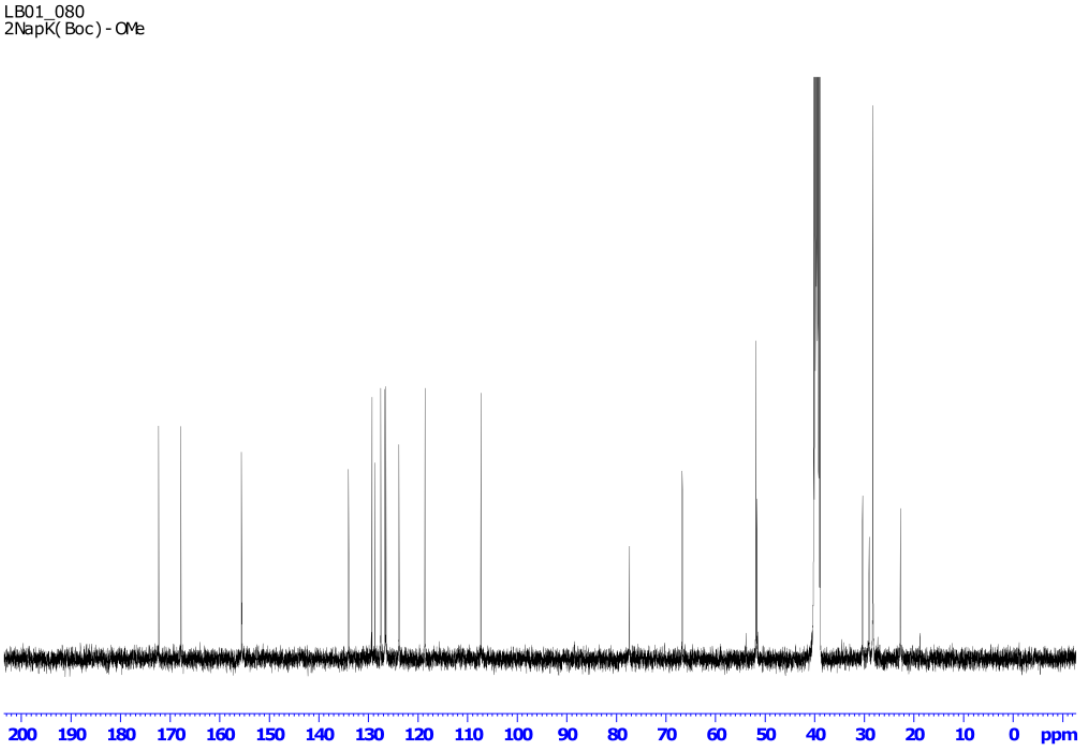

Figure S51. ^{13}C NMR of 2NapK(Boc)-OMe in d_6-DMSO at 25°C.

δ_{13C}(100 MHz, DMSO$_{d6}$): 172.30 (C=O), 167.81 (C=O), 155.60 (C=O), 155.53 (ArC), 133.99 (ArC), 129.26 (ArC), 128.71 (ArC), 127.49 (ArC), 126.66 (ArC), 126.45 (ArC), 123.82 (ArC), 118.59 (ArC), 107.31 (ArC), 77.31 (**C**$(CH_3)_3$), 66.68 (2Nap-OCH_2), 51.86 (COO**C**H_3), 51.63 (*CH), 39.50 (septet, d_6-DMSO), 39.27 (*CH**C**H_2) 30.31 (CH_2), 28.99 (CH_2), 28.23 (C(**C**$H_3)_3$, 22.67 (CH_2).

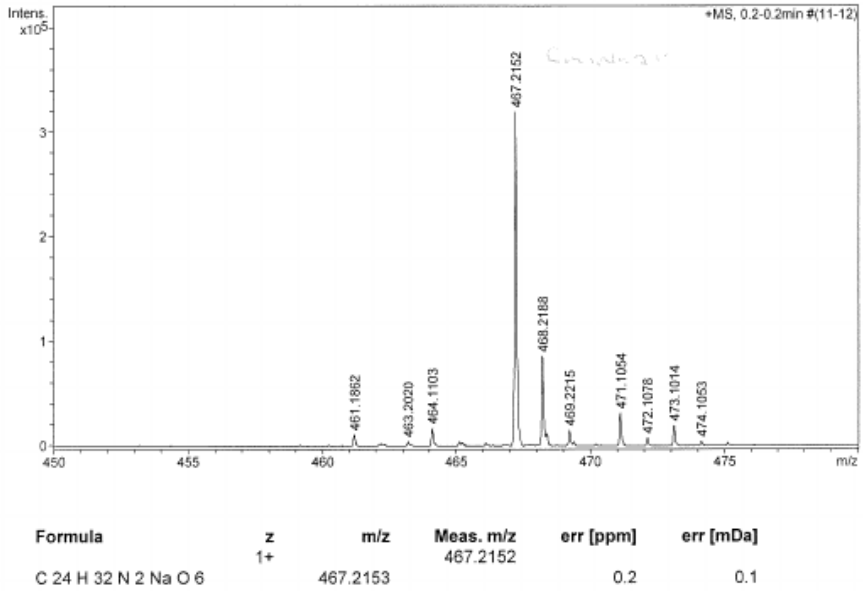

Figure S52. Mass spectrum of 2NapK(Boc)-OMe. **HRMS (ESI) m/z: ([M$^+$Na]$^+$).** Accurate Mass calculated for $C_{24}H_{32}N_2NaO_6$: 467.2153. Found: 467.2152

2NapK(Boc)

(a)

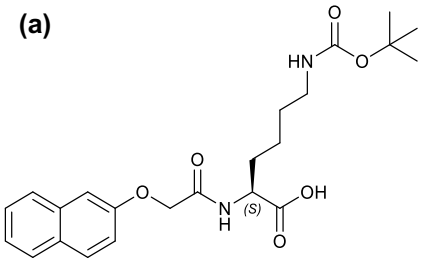

(b)

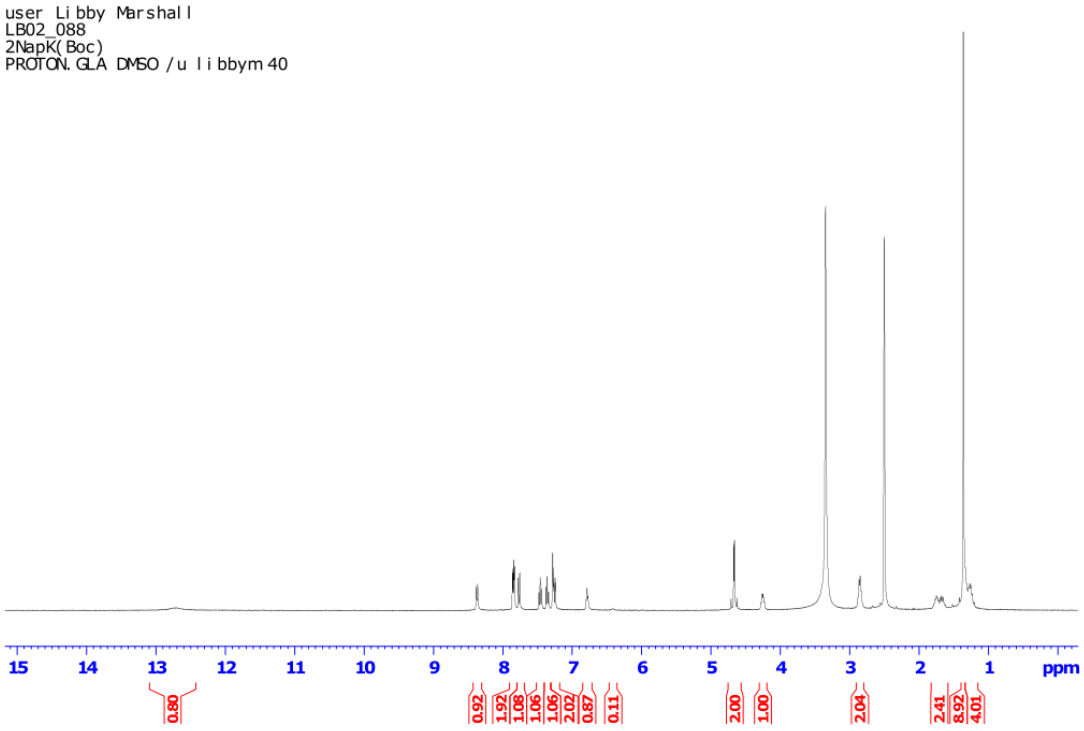

Figure S53. (a) Chemical structure of 2NapK(Boc), product of the methyl ester deprotection of 2NapK(Boc)-OMe, (b) ^{1}H NMR of 2NapK(Boc) in *d*$_6$-DMSO at 25°C.

δ_H(400 MHz, DMSO$_{d6}$): 12.73 (1H, s, COOH), 8.37 (1H, d, *J* = 7.8 Hz, NH), 7.86-7.83 (2H, m, ArH), 7.78-7.76 (1H, m, ArH), 7.48-7.44 (1H, m, ArH), 7.38-7.34 (1H, m, ArH), 7.29-7.24 (2H, m, ArH), 6.80-6.77 (1H, m, NH-Boc), 4.66 (2H, dd, *J* = 14.7, 14.7 Hz, Nap-OCH$_2$), 4.28-4.23 (1H, m, *CH), 3.35 (s, H$_2$O), 2.88-2.83 (2H, m, CH$_2$), 2.50 (q, *d*$_6$-DMSO)1.80-1.62 (2H, m, CH$_2$), 1.36 (9H, s, (CH$_3$)$_3$), 1.33-1.20 (4H, m, CH$_2$).

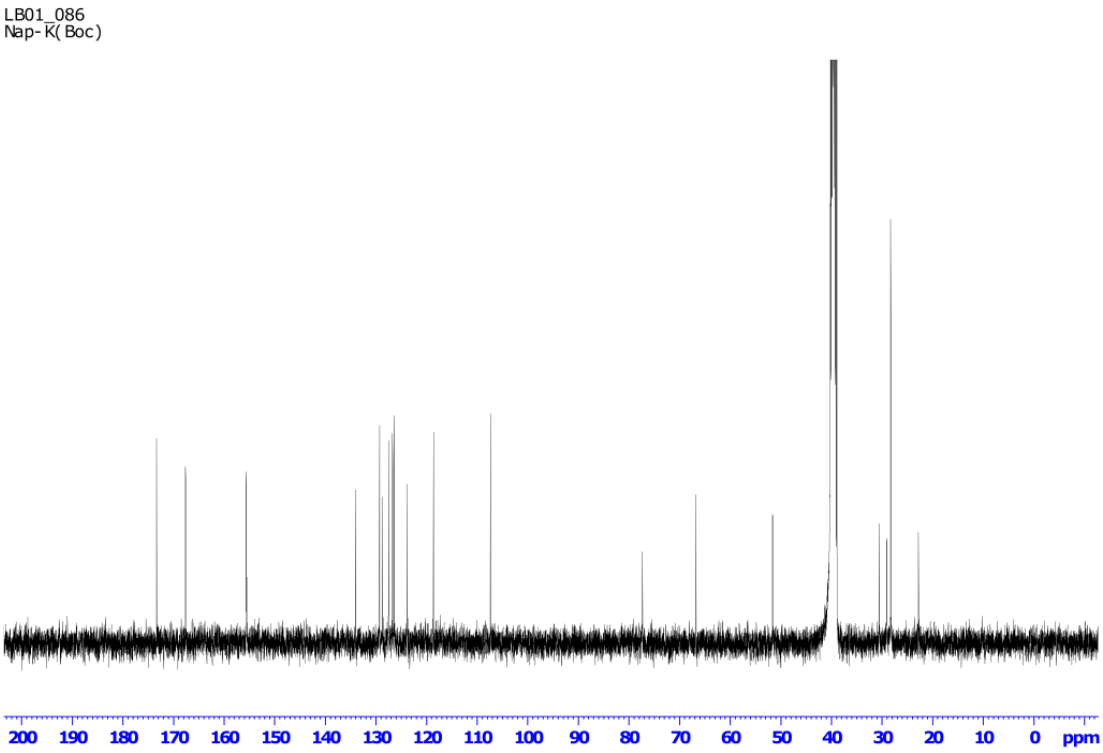

Figure S54. ^{13}C NMR of 2NapK(Boc) in d_6-DMSO at 25°C.

δ_{13C}(100 MHz, DMSO$_{d6}$): 173.34 (C=O), 167.61 (C=O), 155.60 (C=O), 155.54 (ArC), 134.01 (ArC), 129.26 (ArC), 128.70 (ArC), 127.48 (ArC), 126.70 (ArC), 126.42 (ArC), 123.81 (ArC), 118.60 (ArC), 107.33 (ArC), 77.31 ($C(CH_3)_3$), 66.73 (2Nap-OCH_2), 51.57 (*CH), 39.50 (septet, d_6-DMSO), 39.23 (CH_2), 30.51 (CH_2), 29.04 (CH_2), 28.24 ($C(\mathbf{C}H_3)_3$, 22.75 (CH_2).

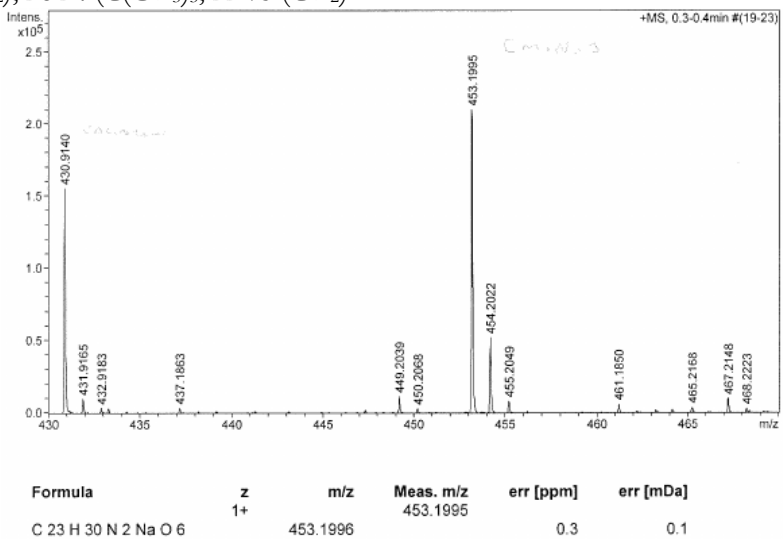

Formula	z	m/z	Meas. m/z	err [ppm]	err [mDa]
	1+		453.1995		
C 23 H 30 N 2 Na O 6		453.1996		0.3	0.1

Figure S55. Mass spectrum of 2NapK(Boc). **HRMS (ESI) m/z: ([M$^+$Na] $^+$):** Accurate Mass calculated for $C_{23}H_{30}N_2NaO_6$: 453.1996. Found: 453.1995.

2NapK(Boc)FF-OMe

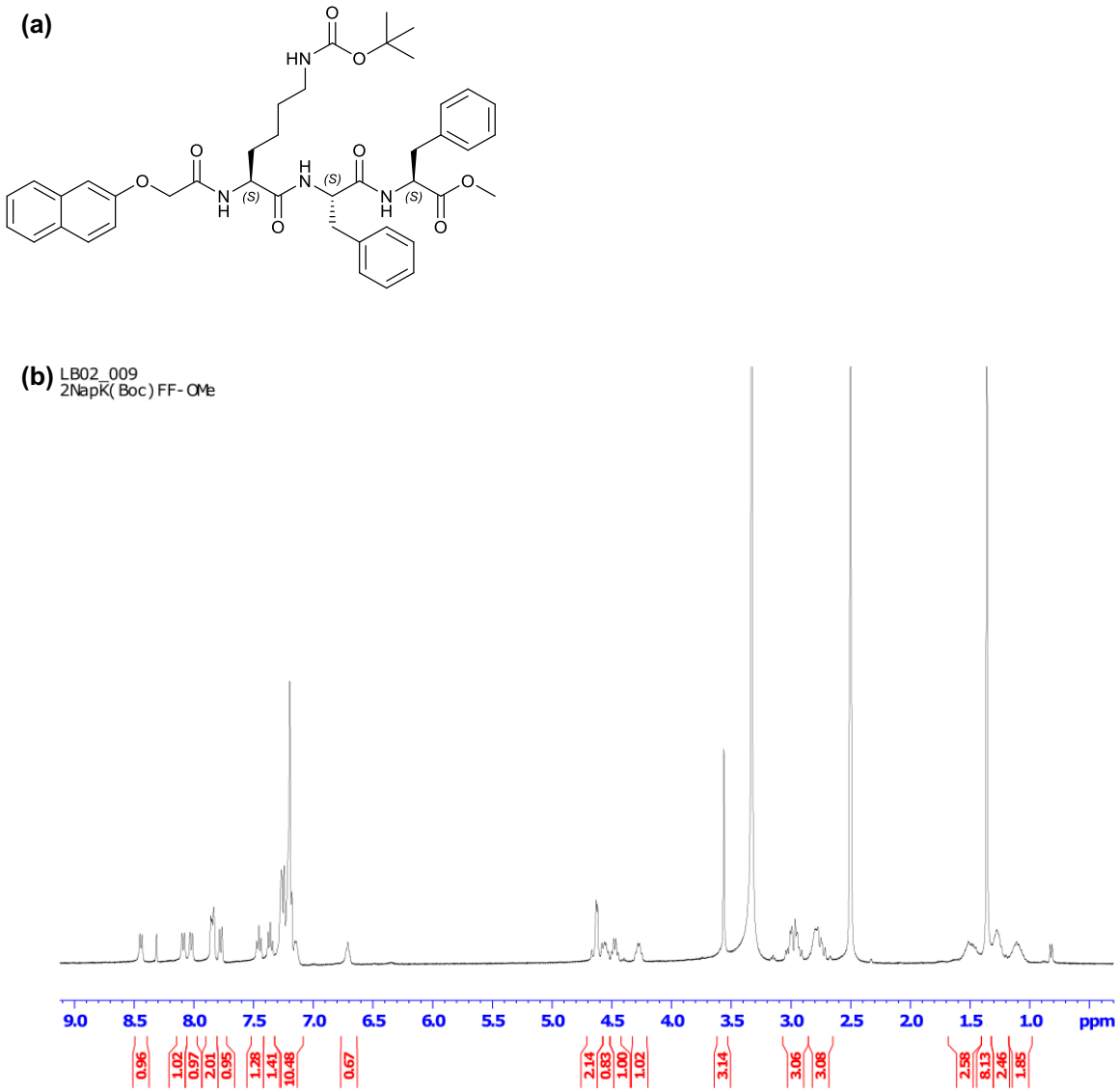

Figure S56. (a) Chemical structure of 2NapK(Boc)FF-OMe, product of the coupling reaction between 2NapK(Boc) and TFA.FF-OMe, (b) ^{1}H NMR of 2NapK(Boc)FF-OMe in *d*$_6$-DMSO at 25°C.

δ_H(100 MHz, DMSO$_{d6}$): 8.44 (1H, d, *J* = 7.2 Hz, NH), 8.31 (s, CH_3Cl), 8.09 (1H, d, *J* = 8.9 Hz, NH), 8.02 (1H, d, *J* = 8.0 Hz, NH), 7.86-7.83 (2H, m, ArH), 7.78-7.76 (1H, m, ArH), 7.47-7.43 (1.3H, m, ArH), 7.38-7.34 (1.4H, m, ArH), 7.27-7.12 (10.5H, m, ArH, NH-Boc), 6.69 (0.7H, m, NH-Boc), 4.67-4.58 (2H, m, 2Nap-OCH_2), 4.58-4.53 (1H, m, *CH), 4.50-4.45 (1H, m, *CH), 4.30-4.24 (1H, m, *CH), 3.56 (3H, s, $COOCH_3$), 3.33 (s, H_2O), 3.04-2.91 (3H, m, CH_2), 2.84-2.71 (3H, m, CH_2), 2.50 (*d*$_6$-DMSO), 1.56-1.45 (2H, m, CH_2), 1.36 (9H, s, $C(CH_3)_3$), 1.30-1.24 (2H, m, CH_2), 1.16-1.03 (2H, m, CH_2).

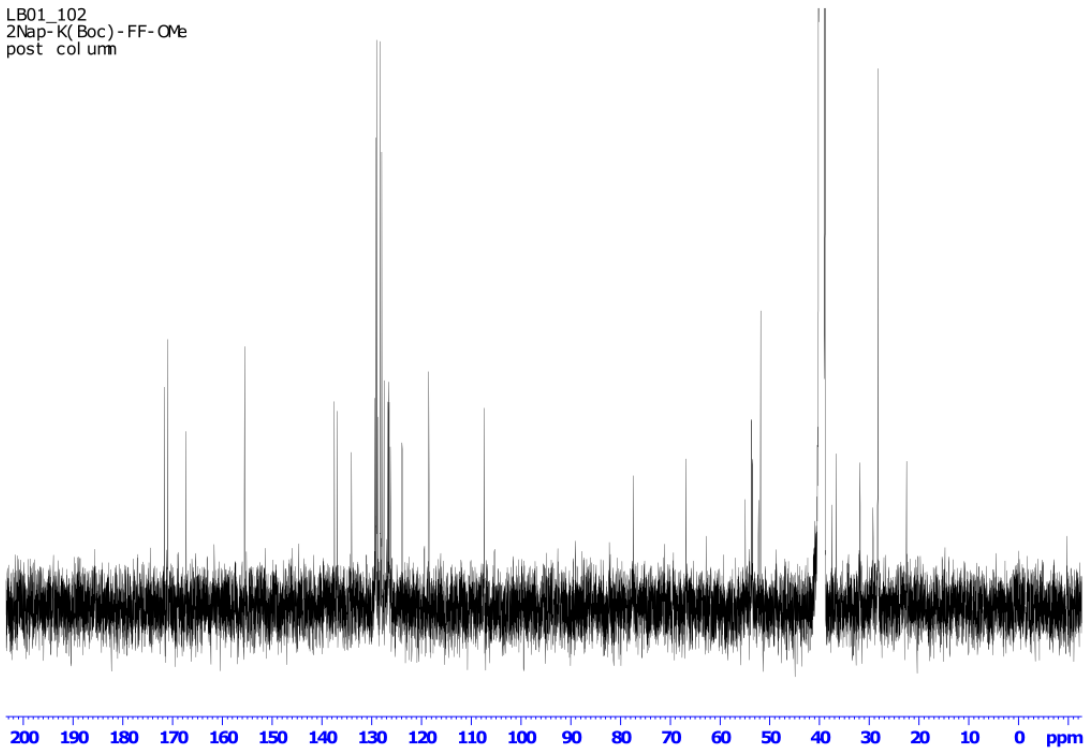

Figure S57. ^{13}C NMR of 2NapK(Boc)FF-OMe in d_6-DMSO at 25°C.

δ_{13C}(100 MHz, DMSO$_{d6}$): 171.65 (C=O), 171.63 (C=O), 171.03 (C=O), 167.32 (C=O), 155.53 (C=O, *overlapping ArC peak not resolved*), 137.49 (ArC), 136.93 (ArC), 134.04 (ArC), 129.38 (ArC), 129.15 (ArC), 129.00 (ArC), 128.75 (ArC), 128.25 (ArC), 127.98 (ArC), 127.51 (ArC), 126.75 (ArC), 126.56 (ArC), 126.48 (ArC), 126.23 (ArC), 123.88 (ArC), 118.50 (ArC), 107.36 (ArC), 77.34 (**C**$(CH_3)_3$), 66.78 (Nap-OCH_2), 54.89, 53.63 (*CH), 53.42 (*CH), 52.23 (*CH), 51.81 (*CH), 39.50 (septet, d_6-DMSO), 39.0 (*CH**C**H_2), 37.43 (CH_2), 36.60 (CH_2), 31.83 (CH_2), 29.21 (CH_2) 28.26 (C(**C**$H_3)_3$), 22.47 (CH_2).

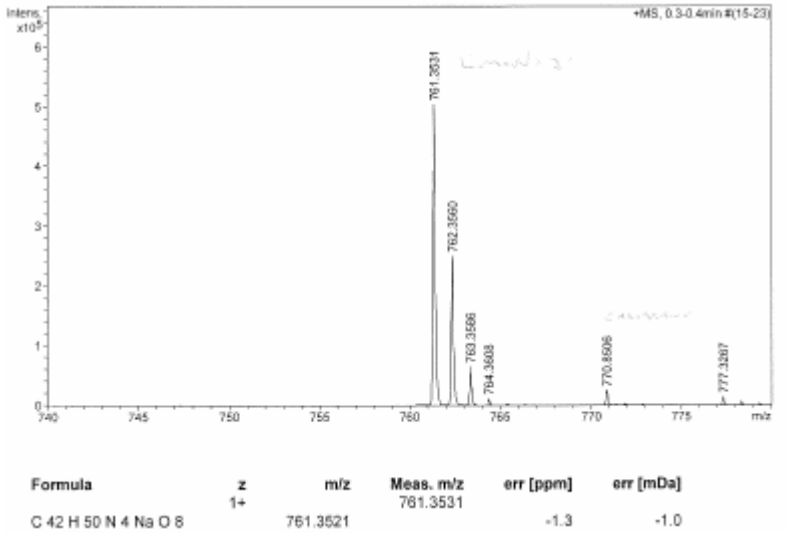

Figure S58. Mass spectrum of 2NapK(Boc)FF-OMe. **HRMS (ESI) m/z: ([M$^+$Na]$^+$).** Accurate Mass calculated for $C_{42}H_{50}N_4NaO_8$: 761.3521. Found: 761.3531.

2NapK(Boc)FF

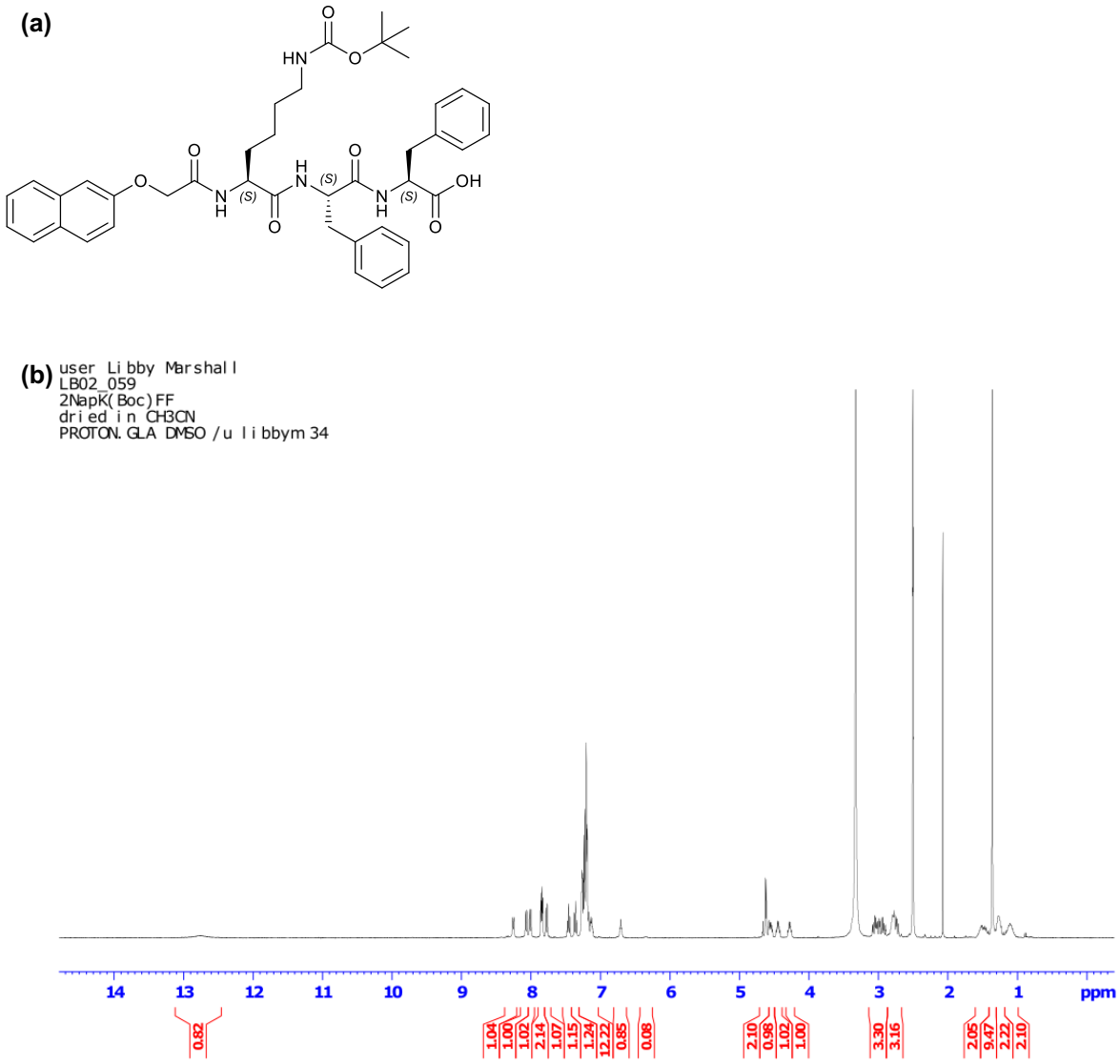

Figure S59. (a) Chemical structure of 2NapK(Boc)FF, product of methyl ester deprotection of 2NapK(Boc)FF-OMe, (b) ^{1}H NMR of 2NapK(Boc)FF in *d*$_6$-DMSO at 25°C.

δ_H(400 MHz, DMSO$_{d6}$): 12.75 (1H, s, COOH), 8.25 (1H, d, *J* = 7.6 Hz, NH), 8.07 (1H, d, *J* = 8.4 Hz, NH), 8.01 (1H, d, *J* = 8.3 Hz, NH), 7.86-7.83 (2H, m, ArH), 7.78-7.76 (1H, m, ArH), 7.48-7.44 (1H, m, ArH), 7.38-7.34 (1H, m, ArH), 7.28-7.10 (12H, m, ArH), 6.72-6.69 (1H, m, NH-Boc), 4.62 (2H, dd, *J* = 14.7, 14.7 Hz, Nap-OCH$_2$), 4.57-4.52 (1H, m, *CH), 4.47-4.42 (1H, m, *CH), 4.30-4.25 (1H, m, *CH), 3.33 (s, H$_2$O), 3.08-2.89 (3H, m, CH$_2$), 2.82-2.71 (3H, m, CH$_2$), 2.50 (q, *d*$_6$-DMSO), 1.58-1.41 (2H, m, CH$_2$), 1.36 (9H, s, C(CH$_3$)$_3$), 1.31-1.20 (2H, m, CH$_2$), 1.17-1.03 (2H, m, CH$_2$).

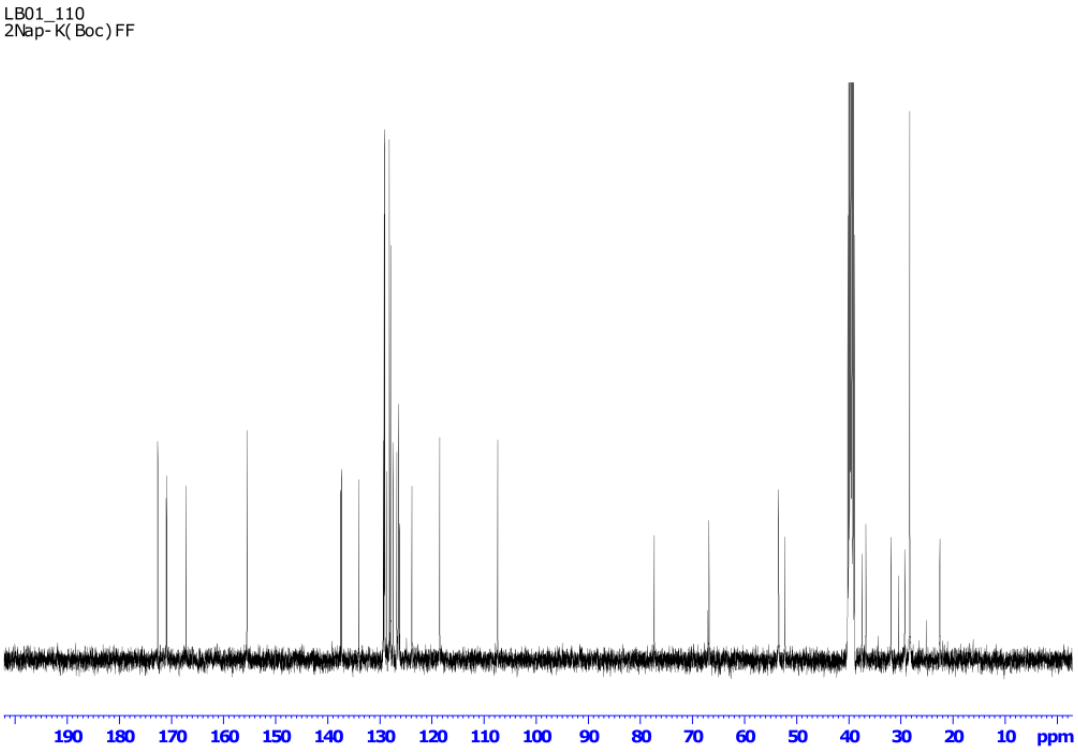

Figure S60. ^{13}C NMR of 2NapK(Boc)FF in d_6-DMSO at 25°C.

δ_{13C}(100 MHz, DMSO$_{d6}$): 172.63 (C=O), 170.98 (C=O), 170.90 (C=O), 167.21 (C=O), 155.51 (C=O), 137.56 (ArC), 137.30 (ArC), 134.02 (ArC), 129.34 (ArC), 129.16 (ArC), 129.06 (ArC), 128.72 (ArC), 128.15 (ArC), 127.91 (ArC), 127.48 (ArC), 126.72 (ArC), 126.44 (ArC), 126.40 (ArC), 126.16 (ArC), 123.83 (ArC), 118.48 (ArC), 107.35 (ArC), 77.28 (**C**$(CH_3)_3$), 66.78(Nap-OCH_2), 53.45 (*CH), 53.41 (*CH), 52.17 (*CH), 39.50 (septet, d_6-DMSO), (37.42 (CH_2), 36.66(CH_2), 31.84 (CH_2), 30.40 (CH_2), 29.21 (CH_2), 28.24 C$(CH_3)_3$, 22.46 (CH_2).

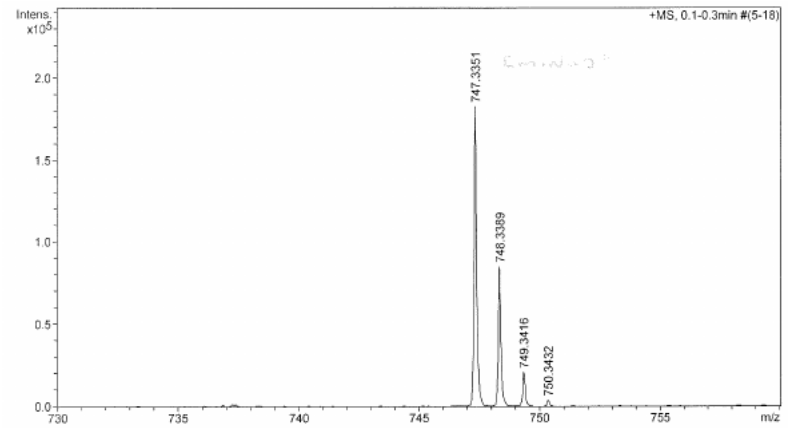

Formula	z	m/z	Meas. m/z	err [ppm]	err [mDa]
	1+		747.3351		
C 41 H 48 N 4 Na O 8		747.3364		1.8	1.3

Figure S61. Mass spectrum of 2NapK(Boc)FF. **HRMS (ESI) m/z: ([M$^+$Na]$^+$).** Accurate Mass calculated for $C_{41}H_{48}N_4NaO_8$: 747.3364. Found: 747.3351.

2NapKFF

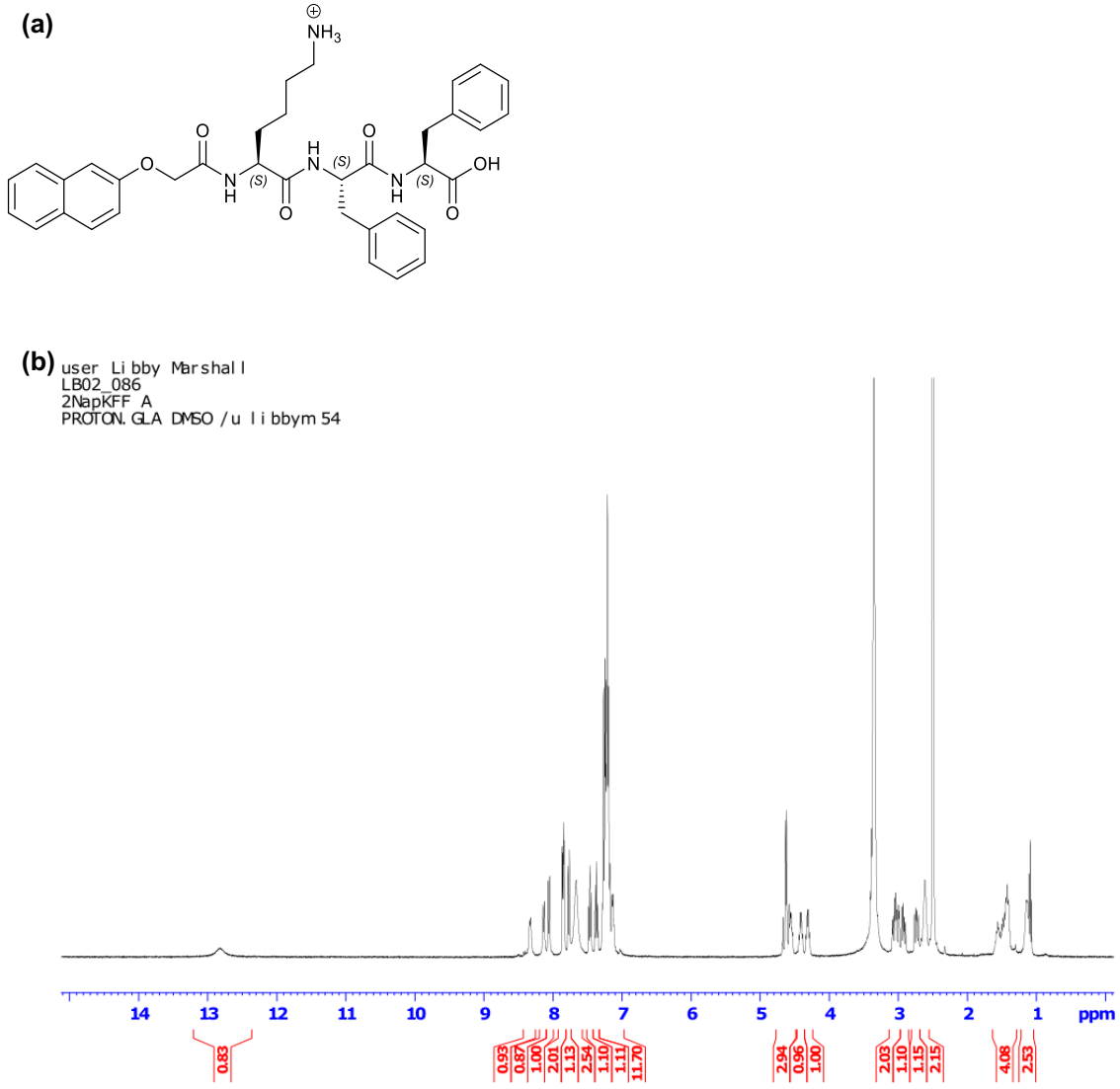

Figure S62. (a) Chemical structure of 2NapKFF, product of Boc deprotection of 2NapK(Boc)FF, (b) ^{1}H NMR of 2NapKFF in *d*$_6$-DMSO at 25°C.

δ_H(400 MHz, DMSO$_{d6}$): 12.82 (1H, s, COOH), 8.33 (1H, d, *J* = 7.2 Hz, NH), 8.10 (1H, d, *J* = 8.1, NH), 8.06 (1H, d, *J* = 8.3 Hz, NH), 7.87-7.84 (2H, m, ArH), 7.78-7.76 (1H, m, ArH), 7.67 (3H, s, NH_3^+), 7.49-7.45 (1H, m, ArH), 7.39-7.35 (1H, m, ArH), 7.29-7.11 (12H, m, ArH), 4.63 (2H, dd, *J* = 14.7, 14.5 Hz, Nap-OCH_2), 4.58-4.53 (1H, m, *CH), 4.44-4.38 (1H, m, *CH), 4.34-4.28 (1H, m, *CH), 3.35 (s, H_2O), 3.09-2.90 (2H, m, *CHC**H**$_2$), 2.92 (1H, dd, *J* = 13.8, 8.6, *CHC**H**$_2$), 2.74 (1H, dd, *J* 13.8, 9.8, *CHC**H**$_2$), 2.67-2.57 (2H, m, C**H**$_2$-NHBoc), 2.50 (*d*$_6$-DMSO), 1.61-1.38 (4H, m, CH_2), 1.18-1.07 (2H, m, CH_2), purity: 99%.

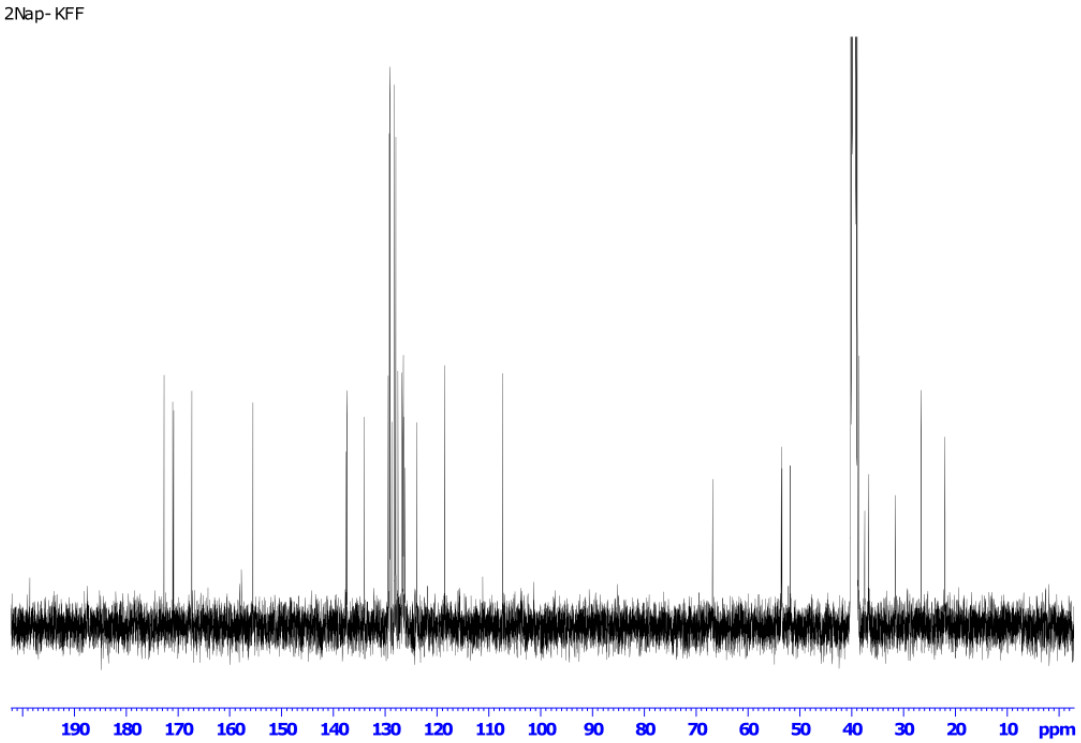

Figure 63. ^{13}C NMR of 2NapKFF in d_6-DMSO at 25°C.

δ_{13C}(100 MHz, DMSO$_{d6}$): 172.64 (C=O), 170.98 (C=O), 170.80 (C=O), 167.28 (C=O), 155.57 (ArC), 137.53 (ArC), 137.36 (ArC), 134.00 (ArC), 129.38 (ArC), 129.17 (ArC), 129.08 (ArC), 128.73 (ArC), 128.17 (ArC), 127.92 (ArC), 127.51 (ArC), 126.70 (ArC), 126.49 (ArC), 126.42 (ArC), 126.18 (ArC), 123.89 (ArC), 118.49 (ArC), 107.32 (ArC), 66.77 (Nap-OCH_2), 53.51 (*CH), 53.39 (*CH), 51.82 (*CH), 38.62 (CH_2), 37.42 (CH_2), 36.64 (CH_2), 31.50 (CH_2), 26.58 (CH_2), 21.95 (CH_2).

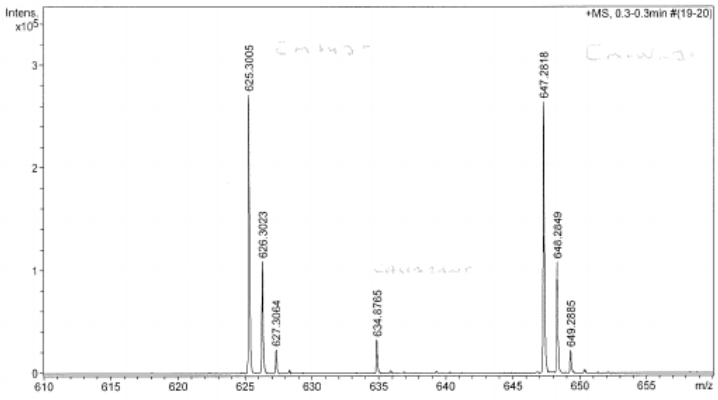

Formula	z	m/z	Meas. m/z	err [ppm]	err [mDa]
C 36 H 41 N 4 O 6	1+	625.3021	625.3005	2.4	1.5
C 36 H 40 N 4 Na O 6	1+	647.2840	647.2818	3.4	2.2

Figure S64. Mass spectrum of 2NapKFF. **HRMS (ESI) m/z: ([M$^+$Na]$^+$).** Accurate Mass calculated for $C_{36}H_{40}N_4NaO_6$: 647.2840. Found: 647.2818.

1. L. Chen, K. Morris, A. Laybourn, D. Elias, M. R. Hicks, A. Rodger, L. Serpell and D. J. Adams, *Langmuir*, 2010, **26**, 5232-5242.
2. A. M. Fuentes-Caparros, Z. Canales-Galarza, M. Barrow, B. Dietrich, J. Lauger, M. Nemeth, E. R. Draper and D. J. Adams, *Biomacromolecules*, 2021, **22**, 1625-1638.
3. O. Arnold, J. C. Bilheux, J. M. Borreguero, A. Buts, S. I. Campbell, L. Chapon, M. Doucet, N. Draper, R. F. Leal, M. A. Gigg, V. E. Lynch, A. Markvardsen, D. J. Mikkelson, R. L. Mikkelson, R. Miller, K. Palmen, P. Parker, G. Passos, T. G. Perring, P. F. Peterson, S. Ren, M. A. Reuter, A. T. Savici, J. W. Taylor, R. J. Taylor, R. Tolchenoy, W. Zhou and J. Zikoysky, *Nuclear Instruments & Methods in Physics Research Section a-Accelerators Spectrometers Detectors and Associated Equipment*, 2014, **764**, 156-166.
4. www.sasview.org.